Copy 3 - w 396

SEISMIC ANALYSIS OF THE FATIH SULTAN MEHMET (SECOND BOSPORUS) SUSPENSION BRIDGE

A A Dumanoglu
Karadeniz Technical University, Department of Civil Engineering, Trabzon, Turkey

J M W Brownjohn and R T Severn
University of Bristol, Queen's Building, Bristol BS8 1TR, UK

SUMMARY

Theoretical dynamic characteristics of the Fatih Bridge in terms of natural frequencies and mode shapes of free vibration were obtained using a range of finite element models. Based on this free vibration data, separate analyses of the asynchronous response of the bridge to earthquake excitation in three orthogonal axes with different speeds of wave propagation, and of stochastic response to vertical excitation were used to estimate levels of dynamic response due to seismic loading.

Fatih is the third of three modern European long span suspension box-girder suspension bridges that have been investigated and the relationship of the different design features and the dynamic responses of this type of bridge is reviewed.

The main conclusion is that where seismic response is an important consideration, the effects of asynchronous excitation can be significant and must be considered.

INTRODUCTION

The study described here is the continuation of the research work[1-6] which has been carried out on modern European long span box-girder suspension bridges, specifically the Humber and Bogazici (first Bosporus) bridges. In these previous research works, dynamic characteristics in terms of natural frequencies, mode shapes and damping ratios were determined by combinations of theoretical investigations and prototype testing on the actual structures. These studies have provided information for the correct mathematical modelling used for dynamic response analyses in the later stage of the response calculations[1-5] for asynchronous and stochastic loading processes.

The aim of this research work is similar to that of previous work in determining dynamic properties of the Fatih Bridge and using these properties in comprehensive asynchronous and stochastic response analyses.

DESCRIPTION OF THE BRIDGE

Construction of the Fatih Bridge[7] (fig. 1) was part of a major program of construction of a second peripheral highway around Istanbul, and the Bridge was opened to traffic in 1989. It has a box girder deck 39.4m wide overall and 1090m long, carrying two 4-lane highways. There are no side spans and the steel towers rise 110m above ground level. The deck roadway is only 8m above foundation level at the towers where an arrangement of rocker and expansion bearings at the deck-tower connection is intended to permit longitudinal translation of the deck and rotation about a lateral axis but to restrict other translations and rotations. The hangers are vertical and connect to the deck and cable with singly hinged bearings. These features, which differ from those of the Bogazici Bridge[8] (similar span but with inclined hangers, approach viaducts and a narrower six-lane deck) lead to a rather different dynamic response.

Table 1 presents details of dimensions, and material and sectional properties for comparison with those of Bogazici and Humber.

MATHEMATICAL MODELLING

The linear mathematical modelling of the bridge, using 'MULSUP' an adaptation of the SAP4 structural analysis program, was based on the assumption that the bridge vibrates around its dead-load state which is accepted as the design configuration.

In order to determine the importance of three-dimensional vibrations in the structure and to check the degree of accuracy required for accurate modelling, the free vibration characteristics were initially determined from three different mathematical models:

1) Two-dimensional, vertical plane
2) Two-dimensional, horizontal plane
3) Three-dimensional

In each model the lateral axis is in the upstream/downstream direction and the longitudinal axis is along the deck.

Two-Dimensional Modelling

The vertical plane model has only three degrees of freedom (DOFs) assigned to each nodal point, these being two translational degrees of freedom in vertical and longitudinal axes and one rotational degree of freedom about the lateral axis. The horizontal plane mathematical model has four degrees of freedom, two for translation in the lateral and longitudinal axes and two for rotation about the vertical and longitudinal axes. This last DOF applies only to the towers where it is necessary for representation of tower bending in lateral vibration.

The bridge structure is represented entirely by beam elements. For the deck these elements have similar bending stiffness, cross sectional area and mass properties to those of the prototype box-girder. Because of the very large axial forces, geometric stiffness matrices are added to the elastic stiffness matrices in forming the elemental stiffness matrices for the main cables, hangers and towers.

In the vertical plane model the hangers are hinged about the lateral axis at both ends. The bearings between the deck and towers are represented as swing links so as to allow free longitudinal motion and rotation about the lateral axis.

Fig. 2 shows the arrangement of nodal points for the two-dimensional model used for vertical plane and lateral analyses; it has 139 nodes 196 elements, with 393 degres of freedom in the vertical plane model.

Three-dimensional Modelling

With six degrees of freedom allowed for each node in this model it is possible to obtain not only vertical and lateral modes but also torsional modes and modes with anti-phase lateral vibration of the main cables.

One of the major differences between the two and three-dimensional mathematical models is in the representation of the box-girder deck, which is now represented by equivalent plate elements with similar bending, torsional and membrane properties to those of the box-girder deck. The plate element used in the three-dimensional modelling has six degrees of freedom at each nodal point[1,4].

Fig. 3 shows the arrangement of nodal points for the three-dimensional model; it has 280 nodes 276 beam elements, 61 plate/shell elements and 1586 degrees of freedom.

Boundary conditions

Previous analyses have shown that the free-vibration response, particularly for the lowest vertical modes of the vibration, depends on the nature of the deck boundary conditions, so two variants were devised for each of the three models described above, featuring different restraint at the ends of the deck (fig. 4):

In variant SS the bearings at both ends of the deck are allowed to slide and hinge, by means of a hinged link mechanism, as shown in the left half of fig. 4 for the three-dimensional model.

In variant FS the boundary conditions are changed so that one end is still hinged but is prevented from sliding, as in the right half of fig. 4.

NATURAL FREQUENCIES AND MODE SHAPES

The equations of motion are

$$\mathbf{M}\ddot{\mathbf{x}} + \mathbf{C}\dot{\mathbf{x}} + \mathbf{K}\mathbf{x} = \mathbf{f} \qquad 1)$$

where $\mathbf{M}$, $\mathbf{C}$ and $\mathbf{K}$ are the global mass, damping and stiffness matrices of the bridge, $\mathbf{x}$, $\dot{\mathbf{x}}$ and $\ddot{\mathbf{x}}$ are the displacement, velocity and acceleration vectors of responses and $\mathbf{f}$ is the forcing function. The stiffness matrix $\mathbf{K}$ contains not only the elastic component of the stiffness terms $\mathbf{K_e}$, but also the gravity stiffness matrix representing the contribution of gravity effects, $\mathbf{K_g}$.

The undamped free-vibration response of the bridge is given by

$$\mathbf{M}\ddot{\mathbf{x}} + \mathbf{K}\mathbf{x} = \mathbf{0} \qquad 2)$$

and the natural frequencies ω_r and mode shapes φ_r of the bridge are the values of ω and φ that satisfy the eigenvalue equation obtained from eq. 2:

$$(\mathbf{K} - \omega^2\mathbf{M})\,\varphi = \mathbf{0} \qquad 3)$$

The mode shapes φ_r are mass-normalised so that $\varphi_r^T M \varphi_r = 1$.

Eigensolutions were obtained for the first 20 modes each of the two-dimensional models and for the first 40 modes of the three-dimensional model. The six complete sets of modes can be found in references 9 and 10.

Table 2 summarises the characteristics of the three-dimensional modes up to 1.0Hz which can be arranged into four major types:

Modes in which the deck, towers and cable move longitudinally and/or vertically (V)

Modes in which the deck oscillates in torsion (T)

Modes in which the deck and cable move laterally, usually with participation of the tower pylons and in-phase cable motion (L,C^+,P)

Modes in which the cables move laterally in anti-phase with minimal participation of the tower and deck (C^-)

Fig. 5 shows the mode shapes for the twelve lowest modes generated by either variant (SS or FS), including an example of each mode type. The upper view for each mode shows only the component of vibration in the vertical plane, the lower view shows only the horizontal component.

Table 2 also specifies the number of nodes in the modal shapes for the deck and cables (not always the same for the same mode), indicates which modes are specific to only one of the two variants and shows frequencies obtained from the equivalent two-dimensional model for vertical modes. Although the cable motion in the three-dimensional solution complicates direct comparison, some equivalent two-dimensional lateral modes are indicated.

The vertical modes show the usual progression of nodes and have limited longitudinal participation of the tower pylons (because of the stiffness of the back stay cables). The torsional modes also show a clear progression and also involve limited twisting of the pairs of tower pylons.

With the exception of C^- modes where vibrations are confined to anti-phase motion of the main cables (e.g. mode 10) the lateral modes involve varying degrees of motion of the deck and towers. Where pairs of lateral modes appear with apparently the same mode shape (modes 7 and 13; 23 and 26; 40 and 41) for the higher mode of each pair the phase of the cable motion is opposite to that of the deck motion for the greater part of the span.

The frequency for the first vertical mode has increased slightly from 0.108Hz for the SS variant to 0.125Hz for the FS variant due to the longitudinal restraint and mode 4, which has a high degree of longitudinal motion, disappears in the FS variant. For most higher modes there is no significant difference except for mode 37 which is an axial

vibration of the deck restrained at one end in the FS variant. The significance of this result is that for a bridge with vertical hangers the pendular motion of the deck which might be expected is restrained when the boundary conditions are changed from hinged/sliding to hinged/fixed at one end although both possible first antisymmetric vertical modes occur before the first symmetric mode. For bridges with inclined hangers and similar deck bearings (e.g. Bogazici, Humber)[1] the first symmetric mode is sandwiched between the two possible antisymmetric modes.

Comparison of results from the two- and three- dimensional models shows that apart from the torsional modes, the significant motion of the deck and towers in the vertical and horizontal planes is adequately represented in the respective two-dimensional models, there being only small differences in the natural frequencies due primarily to the reduced freedom in these models. Because the differences are small, the use of computationally more efficient two-dimensional models was justified for the analyses of the separate effects of vertical, lateral and longitudinal ground motion described here. Also, although the true character of the boundary conditions was uncertain at the time of the analysis (done before the prototype testing) the SS variant was used. This was justified by the belief that even if the bearings 'stick' in the FS mode for low levels of vibration (such as observed at Humber) the bearings are likely to function in the SS mode (as for Bogazici) for the large displacements induced by earthquakes.

Validation of natural frequencies and mode shapes

An ambient vibration survey of Fatih Bridge[10,11] has been done to confirm the eigensolutions of the mathematical models. While there were some difficulties in the measurements, they have confirmed the accuracy of the mathematical modelling in respect of the modes of vibration that are significant for these analyses.

DYNAMIC RESPONSE TO VERTICAL ASYNCHRONOUS INPUT

Introduction

For long span structures, the variability of earthquake ground motion between the spatially separated supporting points can produce an extra level of response which is significant in comparison with the dynamic response to uniform support excitation. This problem has been studied by a number of authors[12-14], and notably by Abdel Ghaffar and Stringfellow for truss-girder suspension bridges [15,16]. This part of the paper presents the last of a series of asynchronous excitation studies on the so-called 'modern' type of suspension bridge more common in Europe which has the aerodynamic deck and slender more flexible towers.

The Fatih bridge ranks among the world's longest spans, at 1090m, so that effect of the finite velocity of travelling ground waves can be significant. In order to study the effect of the asynchronicity of inputs on the seismic response, the bridge was analysed

for response to travelling ground motion in each of the vertical, longitudinal and lateral directions using as input the S16E component of the Pacoima Dam record from the 1971 San Fernando Earthquake. The same earthquake record was used to represent both lateral and longitudinal acceleration but the acceleration values were multiplied by a factor of 2/3 to simulate the vertical component. Fig. 6 shows how, for the 3/3 record, the acceleration power spectral density and the displacement response spectrum for 2.5% damping (as used in the analyses) relate to the computed vertical natural frequencies of the bridge up to 5Hz. The actual values determined experimentally[10,11] are different at the higher frequencies, but because it has only been necessary to use the lowest fifteen modes (0-1.1Hz) for convergence of the time history solutions, the errors are not significant.

In the analyses the ground motion was assumed to travel from Europe to Asia (right to left in the figures that follow) with speeds of 250, 500, 1000, 2000 m/second and infinite velocity, the latter equivalent to conventional synchronous analysis.

The method of calculation of responses to travelling ground motion are explained in detail elsewhere[1-3]; only the final expressions are given here. Because of the nature of the problem, displacements have to be calculated in terms of total displacements which have two components; the pseudo-static response and the dynamic response. The vector of total responses may be expressed as

$$\mathbf{v}(t) = \sum_j \mathbf{r}_j v_{jg}(\tau_j, t) \quad + \quad \sum_i \varphi_i Y_i(t) \qquad 4)$$

(pseudo-static) (dynamic)

where $\mathbf{r}_j$ is the displacement shape function (r-vector) due to unit displacement assigned to ground degree of freedom j,

v_{jg} is the ground displacement at degree of freedom j,

τ_j is the arrival time of the ground motion at specific support point j and

Y_i is modal amplitude for mode i.

The pseudo-static response derives from considering the static (massless) response of the structure to unit displacement at a single support degree of freedom (DOF) which gives the r-vector for that DOF, and summing all these effects in proportion to the ground motion at these DOFs. The dynamic part of the response uses as a forcing function a vector of inertia forces that depends on mass distribution scaled by the r-vectors and the support motion. For uniform input this reduces to a uniform body force.

The internal forces in the structure may be calculated by multiplying eq. 4 by the relevant stiffness matrix for each element e.g.

$$\mathbf{p} = \mathbf{K}\mathbf{v} \qquad 5)$$

In this study the absolute maximum value from the time history of each response parameter has been extracted and presented. Because the maxima of pseudo-dynamic and dynamic displacements generally occur at different instants in the time histories the maxima of total displacements will not necessarily be the sum of the maxima of pseudo-static and dynamic components.

Displacements

Fig. 7a,b,c respectively show maxima of pseudo-static, dynamic and total vertical displacements of the deck.

The peak pseudo-static displacements for infinite velocity (fig. 7a, solid line) equate to the peak ground displacement for the earthquake record; the peak displacements generally increase as velocity decreases. Fig. 7b shows the dynamic components of the vertical absolute displacements which are broadly similar for asynchronous and conventional (infinite velocity) analyses. Fig. 7c shows the vertical total displacements of the deck for various velocities which have a maximum of 81cm occurring in the European half of the bridge for the 500m/second wave velocity.

There is not a definite pattern to the relationship between displacements and wave velocity and the results from the conventional analysis appear to be within the limits defined by the other velocities.

Fig. 8 shows longitudinal displacement response for the Asian tower (the results for the European tower are similar). The situation differs from that in the deck since the tower pseudo-static displacements are much larger than the dynamic displacements (figs. 8a,b) so that the total displacements (fig. 8c) for the 250m/second earthquake are approximately three times those obtained with conventional analyses.

Bending Moments

There is little variation in the minimum and maximum values of deck bending moments for different wave velocities, although the bending moments for a wave velocity of 250 m/second are generally the largest, reaching a value of 46MNm at the quarter span position. The maximum bending moment for the conventional analysis occurs at the centre of the span with a value of 36.5MNm.

The effect of the various velocities on the bending moments in the towers (fig. 9; European tower) is more pronounced, with moments generally increasing for decreasing velocity and ranking of values for the different velocities similar to those for tower displacements. While the conventional analysis determines a bending moment of 13.5MNm at the bottom of both towers, the same location in the European and Asian towers experiences bending moments of 52.5MNm for the 250m/second wave velocity. This is due to the pseudo-static components of the response.

Displacement Time-Histories

Fig. 10 shows time-histories of vertical displacement at the mid-point of the deck for 500m/second wave velocity. Even though the bridge has very low natural frequencies, it still has significant response for earthquake motion which contains energy at higher frequencies. After the termination of the earthquake (13.5 seconds) the pseudo-static component is zero but the dynamic components of response quantities decay slowly and the bridge vibrates freely with initial displacement exceeding 65cm.

DYNAMIC RESPONSE TO ASYNCHRONOUS LONGITUDINAL INPUT

Analysis of Humber and Bogazici bridges for asynchronous response to lateral and longitudinal input[3] showed that the resulting displacements and bending moments can be more significant than those for vertical input, and so the exercise was repeated for Fatih.

Displacements

Absolute maxima of pseudo-static, dynamic and total vertical displacements of the deck due to the longitudinal component of travelling ground motion are shown in figs. 11a,b,c respectively.

The pseudo-static components of the vertical displacements are zero for infinite wave velocity, and have a maximum, 108cm at the centre span, for the 500m/second velocity. With the exception of the 500m/second case the displacements reduce with decreasing wave velocity. A likely explanation for this is that for this earthquake record the 500m/second velocity may cause towers to have antiphase motion with increased displacement at centre span occurring when the towers move towards each other. This was found to be the case for the Bogazici Bridge[2].

Dynamic vertical displacements due to the conventional analysis are very small with a negligible value at the centre of the deck, whereas the 500m/second earthquake produces the largest displacements, 364cm, at the same location. Time-wise addition of dynamic and pseudo-static components leads to a maximum displacement of 338cm.

Fig. 12 shows longitudinal displacements in the European tower. Clearly the variations of pseudo-static displacements are very small. This may be explained by the fact that the main cables between the towers are very flexible by comparison with the towers so that longitudinal pseudo-static motions are directly transferred to the tower tops with very little effect due to other parts of the bridge. More significant bending of towers is due to the dynamic effect, with maximum displacement for the 500m/second velocity case.

Bending Moments

The ranking of deck bending moments follows that of the displacements, with a maximum of 80MNm at centre span for the 500m/second case. Fig. 13 shows tower bending moments, again showing bending moments that generally increase for decreasing wave velocity.

DYNAMIC RESPONSE TO ASYNCHRONOUS LATERAL INPUT

Displacements

Absolute maxima of pseudo-static, dynamic and total lateral displacements of the deck due to the lateral component of travelling ground motion are shown in figs. 14a,b,c respectively.

Maxima of pseudo-static displacements are greatest (29.8cm) at the ends of the deck and for infinite lateral wave velocity, and generally decrease for decreasing wave velocity. The maxima of dynamic displacements are generally lowest for the 250m/second case. Over most of the span the total displacements are greatest (55cm) for the 500m/second case and lowest for the infinite velocity case.

For the towers the pseudo-static displacements have almost the same constant value through the height of the tower and for each velocity i.e. they are almost equal to the ground displacement (maximum about 30cm). Dynamic displacements are very small, within the range of 0-0.05cm which may be explained by the rigidity of the towers in the lateral plane compared to the rest of the structure.

Bending Moments

There is no clear relationship between the deck bending moments and wave velocities but the 2000m velocity produces the largest response, at 640MNm.

Fig. 15 shows the tower bending moments which increase almost linearly from tower tip to tower base, rather like a cantilever subjected to a point load. The load here is the inertia forces of the deck transferred to the tower by the cable.

STOCHASTIC RESPONSE TO UNIFORM EXCITATION

For the conventional and asynchronous analyses described above only the instantaneous maximum values and/or their time histories of response quantities can be determined, and basing design on these values can be over-conservative and expensive. The values are for a particular earthquake and do not provide any information about the frequencies of occurrence and average values of these maxima or root mean square (RMS) values and although this type of information can be obtained by further time-history analysis this is inefficient and impractical.

Stochastic analysis is a simple efficient process that provides information about mean of maxima, RMS values, and frequencies and probabilities of occurrence of maxima, as an integral part of the output of a number of finite element computer programs e.g. STOCAL[17] and is used in specialist programs e.g. PSAP[14], STASY[18].

Although a specific time-history is not the usual form of input to a stochastic analysis, the S16E component of the Pacoima Dam record of San Fernando earthquake (2/3 of fig. 6) has also been used as a basis for characterising the uniform (synchronous) ground motion so that results can be compared to those of time history analyses.

The mathematical basis of the stochastic analysis is given in Appendix 1.

Analysis of Stochastic Responses

RMS and mean of maxima of displacements were first calculated using the stochastic method. Absolute maximum values of response quantities were then calculated using the complete quadratic combination (CQC) method, taking into account the cross correlation coefficients between modes of vibration. Vertical displacements of the deck were also calculated by conventional time-history analysis (infinite wave velocity) and results from all the analyses are compared in fig. 16a for a 13.5 second earthquake, showing that mean of maximum displacements and the maxima of displacements determined by the CQC method and the time-history analysis are very close.

The average frequencies of occurrence of displacements are shown in fig. 16b and are mostly around 0.2Hz, close to the frequency (0.18Hz) obtained from the average period between response maxima obtained with the time history method. The results from the stochastic analysis depend on the period over which the response values are calculated (for the same earthquake) and as for Humber and Bogazici[6] the mean of maxima and RMS values decrease if the earthquake is extended by adding zeros. Fig. 16c shows stochastic responses for 20 and 27 second durations.

Figs. 17a,b show the cumulative probability density function (CDF) of vertical peak response at the centre of the deck and longitudinal peak response at the top of the European tower, respectively. The probability of occurrence of a peak vertical deck response below 100cm is 100% whereas the probability of occurrence of a peak less than 20cm is zero. However, if the duration of the earthquake increases, more and more peak values will appear which shows up in the CDF as increased probability of occurrence of a peak below certain levels. For example the probability of occurrence of a peak below 50cm is 35% for the duration of 13.5 seconds, 70% for 20 seconds and 90% for 27 seconds.

Fig. 18 shows bending moments for the deck as mean of maxima and as determined by the CQC method. The 29MNm value from the CQC compares with the value of

37MNm from the time history analysis. For the towers the maximum bending moment (from the CQC method) is 14.5MNm

DISCUSSION AND COMPARISON WITH ANALYSIS OF HUMBER AND BOGAZICI SUSPENSION BRIDGES

Table 3 summarises results obtained from asynchronous analyses of the Humber, Bogazici and Fatih bridges showing the maximum values of pertinent response quantities and, where possible comparing them with estimates of the maximum permissible values. These estimates, which are based on the material and sectional properties given in Table 1 and simple analyses of beam bending ($m = \sigma_{max} I / y$) and direct stresses ($F = \sigma_{max} A$) should be used only as a guide, since the true maximum permissible values would derive from more detailed analyses and designer's judgement. Displacements and axial tower forces do not appear to be a problem for these inputs.

The response quantities in each bridge for vertical and longitudinal input are directly comparable and even allowing for the 2/3 scaling for vertical input, the response values are in every case greater for longitudinal input. The different responses at Humber and Bogazici have already been commented on[2] and mostly relate to the presence of suspended sidespans at Humber. These tend to restrain the towers and also experience the largest displacements and bending moments in the suspended structure. The significant differences between the responses at Bogazici and Fatih are in the tower response due to the shorter towers at Fatih.

For lateral input, the response quantities are greatest in Humber with the largest deck response values in the side spans. Apart from the much reduced tower bending moments in Fatih, the two Bosporus bridges have broadly similar lateral response.

The figures in brackets are the response values for the infinite velocity (conventional analysis) case as a percentage of the absolute maximum. For vertical input the underestimation of response quantities is largest in the towers, but even so, the bending moments do not approach the estimated maximum permissible values.

Because of the antiphase tower motions induced by longitudinal excitation with certain wave velocities conventional analysis greatly underestimates deck displacements but even though these are quite large, the deck bending moments are below the permissible maxima. For the towers the moments at Bogazici are close to the limit for all wave velocities and exceed the limit for Humber, which was designed without consideration for seismic effects.

For lateral input the deck bending moments are significant and Humber would have problems in an earthquake of this type. Both calculated and permissible tower bending moments in each bridge are calculated with the simplifying and optimistic assumption

that the crossbeams do not shear, which would probably result in the greatest overestimation in the maximum permissible values.

There are several factors that affect the accuracy and relevance of these calculations. Firstly, the analyses use a single Californian earthquake which while not exceptionally severe, does provide some reasonable low frequency displacements (fig. 6). Since the asynchronous effects relate to frequency and displacement content a 'design' earthquake appropriate to the local seismicity would need to be chosen. Secondly, the analysis has made some simplifying assumptions about the structure and the way it behaves in an earthquake, some of which have been discussed above. One very important factor is the damping ratio used, which at 2.5% is an upper bound on values determined experimentally at low levels of response for these bridges, and there is some justification in asserting that damping will remain below this level even for the levels of response predicted here. Thirdly, even though Fatih and Bogazici are in a seismic area, wind is likely to be a bigger threat to stability of the suspended structure.

This really asks more questions than have been answered and the significant result distilled from this work is that conventional seismic analyses can considerably underestimate the seismic responses.

DESIGN CONSIDERATIONS

The aim of this research has been principally to examine the influence of the variable ground motion on the dynamic behaviour of these long span bridges. Although these asynchronous analyses have been specific to one earthquake they have been applied to three bridges and this has suggested several general principles for this type of excitation.

1) For lateral and vertical excitation the deck displacements from the conventional analyses are within the range of values obtained from the asynchronous analyses. Deck motion will be greatest for longitudinal excitation and is governed by the motion of the tower tips, with antiphase motion causing largest deck displacements. Even so, wind (instability and buffeting) is likely to be the main consideration for the deck of such a long span bridge.

2) The towers are the most vulnerable components and the largest bending stresses result from lateral and longitudinal excitation for both conventional and asynchronous analyses. For lateral excitation the stress levels predicted by the two methods are similar while for longitudinal excitation asynchronous excitation leads to considerably higher forces. The authors suggest that to account for asynchronous excitation, designs allow for dynamic tower bending moments approximately four times those predicted by conventional analyses.

3) Principally due to the shorter moment arm and the absence of sidespans, the maximum tower bending moments for Fatih are much less than for the other two bridges, although thetower bending stresses due to cable stretch will be higher[7].From the seismic resistance point of view at least it has been advantageous to obtain the navigational clearance by constructing the towers on higher ground.

4) While suspension bridges have very low natural frequencies and earthquakes have short durations, stochastic analysis is still a useful design tool because it is computationally simple, reduces the dependence on a specific earthquake record and provides a useful alternative measure of the response quantities.

CONCLUSIONS

The free-vibration calculations have shown that while torsional vibration modes and certain type of main cable mode can only be obtained from a full three-dimensional representation, the two-dimensional representations which are computationally more efficient represent the important vertical and lateral modes of vibration with adequate accuracy for the analysis described here.

These calculations have once again shown the relevance of the asynchronous excitation in determining upper bound values when calculating the seismic response of this type of bridge. For Fatih the seismic resistance is enhanced by its short towers and wide deck and the maximum bending moments determined using several simplifying assumptions are well within the estimated permissible limits. The analyses have used a particular earthquake which contains energy at the low frequencies of this bridge but the pseudo-static components, which relate to the peak displacements, dominate much of the response and different time histories would be required to determine the effects of a representative worst-case earthquake.

The time history analyses for Fatih have shown that the asynchronous effects are strongest for the vertical deck displacement due to longitudinal antiphase motion of the towers for certain wave speeds, and in the tower bending moments for longitudinal and vertical excitation.

Asynchronous response analyses are expensive and time consuming and useful statistical values such as absolute maxima, RMS and mean of maximum response values and frequencies of occurrence are easily obtained from stochastic analyses, although the results given here do not show the effect of the asynchronous excitation. For Fatih these values are similar to those obtained with time history analyses which show that such analysis can be reliable even for a very flexible structure with long periods of vibration.

ACKNOWLEDGEMENT

The contribution of data and advice from ACER group is gratefully acknowledged.

Appendix 1 Stochastic Response

The cross spectral moments of a parameter q, from which quantities such as RMS values may be obtained, are defined in terms of the cross spectral density functions of q[17,19,20]:

$$\lambda_{m,ij} = \frac{1}{2\pi}\int_0^\infty \omega^m \, S_{q_{ij}}(\omega)d\omega \qquad 6)$$

where $S_{q_{ij}}(\omega)$ is the cross spectral density function of the response quantity q, i and j indicate the nodal points. When m = 0 and i = j the zeroth spectral moment $\lambda_{0,ij}$ gives the mean square value of q.

When q is a nodal displacement, $S_{q_{ij}}(\omega)$is derived starting from eq. 1 whose Fourier transform is

$$(-\omega^2\mathbf{M} + i\omega\mathbf{C} + \mathbf{K})\mathbf{X}(\omega) = \mathbf{F}(\omega) \qquad 7)$$

or $\mathbf{X}(\omega) = \mathbf{H}(\omega)\mathbf{F}(\omega)$

where $\mathbf{H} = \Phi\mathbf{D}^{-1}\Phi^T$, $\mathbf{D}^{-1} = \text{diag}\{H_r\}$ and $H_r = 1/(-\omega^2 + 2i\zeta_r\omega_r + \omega_r^2)$.

The cross spectral density of nodal displacements is given by

$$S_x(\omega) = X(\omega)X^{*T}(\omega)$$

$$= \overline{\Psi}^T\mathbf{D}^{-1}\Phi^T\mathbf{F}\mathbf{F}^{*T}\mathbf{D}\Phi^{-1*}\overline{\Psi} \qquad 8)$$

where $\overline{\Psi} = \Phi^T$ so that $\overline{\psi}_i$ is a column vector of modal contributions $\overline{\psi}_{ir}$ to the response at node i and * indicates complex conjugate.

For ground acceleration input given by $a_g(t)$ the nodal forces are given by

$$f(t) = a_g(t)\mathbf{M}\delta$$

$$F(\omega) = A_g(\omega)\mathbf{M}\delta \qquad 9)$$

where δ is the direction vector, and by defining $\psi_{ir} = \overline{\psi}_{ir}\varphi_r^T\mathbf{M}\delta$ the cross spectral density of response between points i and j can be written

$$S_{x_{ij}}(\omega) = S_a(\omega)\sum_{r=1}^{m}\sum_{s=1}^{m}\psi_{ir}\,\psi_{js}\,H_r(\omega)\,H_s^*(\omega) \qquad 10)$$

where $S_a(\omega) = A_g(\omega)A_g^*(\omega)$ is power spectral density function of the input ground acceleration and m is the number of modes to consider.

If nodal cross-spectral moments are defined in terms of modal cross-spectral moments i.e.

$$\lambda_{m,ij} = \sum_{r=1}^{M} \sum_{s=1}^{M} \psi_{ir}\, \psi_{js}\, \lambda_{m,rs}\,, \qquad 11)$$

substituting eq. 10 in eq. 6 and defining mth order cross-correlation coefficients

$$\rho_{m,rs} = \lambda_{m,rs}/(\lambda_{m,rr}\,.\,\lambda_{m,ss})^{1/2} \qquad 12)$$

leads to

$$\lambda_{0,ij} = \sum_{r=1}^{m} \sum_{s=1}^{m} \psi_{ir}\, \psi_{js}\, \rho_{0,rs}(\lambda_{0,rr}\lambda_{0,ss})^{1/2} \qquad 13)$$

The RMS value of a response quantity may be obtained from eq. 6:

$$\sigma_R = \sqrt{\lambda_0} \qquad 14)$$

and from eq. 14 the mean of maxima, μ, may be expressed as[19]

$$\mu = p\sqrt{\lambda_0} = p\sigma_R \qquad 15)$$

where p is a 'peak' factor. There are several methods for determining peak factor[21].

The complete quadratic combination (CQC) method[19] can be developed and simplified to calculate the mean of maximum response quantities as

$$\overline{R} = (\sum_{r=1}^{m} \sum_{s=1}^{m} \rho_{0,rs}\, \overline{R}_r \overline{R}_s)^{1/2} \qquad 16)$$

where $\overline{R}$ is the mean of maximum response values to be obtained from the method and $\overline{R}_r$ and $\overline{R}_s$ are the contributions from the rth and sth modes.

Cross-correlation coefficients which appear in eq. 16 are unity for well separated modal frequencies, and decrease as modal frequencies become closely-spaced, as is the case for suspension bridges.

The frequency of occurrence, $\overline{\omega}$, of maxima of response quantities is another useful quantity which may be obtained[17,19,21] from

$$\overline{\omega^2} = \sum_{r=1}^{m} \sum_{s=1}^{m} \omega_r\, \omega_s\, \rho_{2,rs}\, \overline{R}_r\, \overline{R}_s \;\Big/\; \sum_{r=1}^{m} \sum_{s=1}^{m} \rho_{0,rs}\, \overline{R}_r\, \overline{R}_s \qquad 17)$$

Finally, the probability of occurrence of peak values is expressed by the cumulative probability distribution function (CDF)[22].

The stochastic analysis of suspension bridges is described in detail in ref. 19.

REFERENCES

1 A. A. Dumanoglu, R. T. Severn, 'Asynchronous Seismic Analysis of Modern Suspension Bridges Part I: Free Vibration' *Report UBCE-EE-85-2*; 'Part II: Response to Travelling Vertical Ground Motion' *Report UBCE-EE-86-3*; 'Part III: Response to Travelling Longitudinal Ground Motion' *Report UBCE-EE-86-4*; 'Part IV: Response to Travelling Lateral Ground Motion' *Report UBCE-EE-86-5*, University of Bristol, Department of Civil Engineering, 1986.

2 A. A. Dumanoglu, R. T. Severn, 'Seismic Response of Modern Suspension Bridges to Asynchronous Vertical Ground Motion', *Proc. ICE, pt. 2*, **83**, 701-730 (1987).

3 A. A. Dumanoglu, R. T. Severn, 'Seismic Response of Modern Suspension Bridges to Asynchronous Longitudinal and Lateral Ground Motion', *Proc. ICE, pt. 2*, **87**, 73-86 (1989).

4 J. M. W. Brownjohn, A. A. Dumanoglu, R. T. Severn, C. A. Taylor, 'Ambient Vibration Measurements of the Humber Suspension Bridge and Comparison with Calculated Characteristics', *Proc. ICE, Pt. 2*, **83** 561-600 (1987).

5 J. M. W. Brownjohn, A. A. Dumanoglu, R. T. Severn, A. Blakeborough, 'Ambient Vibration Survey of the Bosporus Suspension Bridge', *Earthquake eng. struct. dyn.* **18**, 263-283 (1989).

6 A. A. Dumanoglu, R. T. Severn, 'Stochastic Response of Modern Suspension Bridges to Earthquake Forces', *Earthquake eng. struct. dyn.* **19**, 133-152 (1990).

7 W. C. Brown, E. Hemmi, H. Yamauchi, T. Tanabe, S. Uchira, Y. Edamitsu, 'Second Bosporus Bridge', *Mitsubishi tech. bull.* **177** Sept. 87.

8 W. C. Brown, M. F. Parsons, 'Bosporus Bridge Part 1: History of design', *Proc. ICE, Pt. 1*, **58**, 505-567 (1975).

9 A. A. Dumanoglu, J. M. W. Brownjohn, R. T. Severn, 'Fatih Bridge Part I: Dynamic Characteristics and Seismic Behaviours' *Report UBCE-EE-89-9*, University of Bristol, Department of Civil Engineering, 1989.

10 J. M. W. Brownjohn, A. A. Dumanoglu, R. T. Severn, 'Fatih Bridge Part II: Ambient Vibration Survey' *Report UBCE-EE-90-12*, University of Bristol, Department of Civil Engineering, 1990.

11 J. M. W. Brownjohn, A. A. Dumanoglu, R. T. Severn 'Ambient Vibration Survey of the Fatih Sultan Mehmet (Second Bosporus) Bridge.', *Earthquake eng. struct. dyn.* ibid.

12 S. D. Werner, L. C. Lee, H. G. Wong, M. D. Trifunac, 'Structural Response to Travelling Waves', *J. Struct. Div. ASCE* **105**, 2547 (1979)

13 A. S. Nazmy, A. M. Abdel-Ghaffar, 'Effects of Ground Motion Spatial Variability on the Response of Cable-stayed Bridges.' *Earthquake eng. struct. dyn.* **21**, 1-20 (1992).

14 M. C. Lee, J. Penzien, 'Stochastic Seismic Analyses of Nuclear Power Plant Structures and Piping Systems Subjected to Multiple-support Excitatios' EERC-80/19, Earthquake engineering Research Centre, University of California, Berkeley, CA. June 1980.

15 A. M. Abdel-Ghaffar, R. G. Stringfellow, 'Response of Suspension Bridges to Travelling Earthquake Excitation. Part 1 Vertical Response.' *J. Soil Dyn. Earthquake Engng.*, 3, No. 2, 62 (1984).

16 A. M. Abdel-Ghaffar, R. G. Stringfellow, 'Response of Suspension Bridges to Travelling Earthquake Excitation. Part 2 Lateral Response.' *J. Soil Dyn. Earthquake Engng.*, 3, No. 2, 72 (1984).

17 M. R. Button, A. Der Kiureghian, E. L. Wilson, 'STOCAL, User Information Manual', Department of Civil Engineering, University of California, Berkeley, California, 1981.

18 J. S. Owen, A. Blakeborough, 'A study of the effects of asynchronous seismic excitation on a portal frame and cable-stayed bridge.' *Report UBCE-EE-91-4* , University of Bristol, Department of Civil Engineering, 1991.

19 A. A. Dumanoglu, R. T. Severn, 'Stochastic Response of Suspension Bridges to Earthquake Forces' *Report UBCE-EE-89-9*, University of Bristol, Department of Civil Engineering, 1987.

20 D. D. Pfaffinger, 'Probabilistic Dynamic Analysis with ADINA,' *Comput. struct.* 13, 637-646 (1981).

21 A. Der Kiureghian, 'A Response Spectrum Method for Random Vibration of MDF Systems', *Earthquake eng. struct. dyn.* 9, 419-435 (1981).

22 E. H. Vanmarke, 'On the Distribution of the First-Passage Time for Normal Stationary Random Process', *J. Applied Mechanics, ASME,* 42, 215-219 (1975).

LIST OF FIGURES AND TABLES

Table 1 Structural parameters for Fatih, Bogazici and Humber bridges

	Suspended span dimensions (m)					Tower pylons			Axial area (m^2)		Young's modulus (kN/mm^2)		Second moment of area (m^4)			
	span lengths			depth	width	height	width	length	deck	towers	deck	towers	deck		towers	
	side span 1	main span	side span 2		(overall)	(m)	(m)	(m)					vertical	lateral	longitudinal	lateral
Fatih	(210)[1]	1090	(210)[1]	3	39.4	110.1	3-5	4	1.26	2.4-2.9	205	205	1.73	129	4.32-7.16	772-938
Bogazici	(231)[1]	1074	(255)[1]	3.0	33.4	165	3-5.2	7	0.85	1.36[2]	205	205	1.238	63.6	9.0[2]	292[2]
Humber	280	1410	530	4.5	28.5	155.5	4.5-6	4.75-6	0.73	40.75[2]	200	20	1.94	37.1	132[2]	6497[2]

notes: 1 span lengths in brackets are distances for unsupported side-spans or distances from towers to anchorages

2 axial area and 2nd moment of area figures for towers are average values used in mathematical models

Table 2 Theoretical natural frequencies

Mode			Nodes in ..		3-d model frequency /Hz	2-d model frequency /Hz
no.	type and symmetry		deck	cables		
1	L,C^+ sym		0	0	0.076	0.073
2	V asym	SS	1	1	0.108	0.108
3	V asym	FS	1	1	0.125	0.125
4	V,Long	SS	1	1	0.145	0.144
5	V sym		2	2	0.159	0.159
6	V asym		2	2	0.211	0.212
7	L,C^+ asym, P		1	1	0.232	
8	T sym		0	0	0.243	0.218
9	V sym		3	3	0.250	0.251
10	C^- sym		-	0	0.266	
11	C^- asym		-	1	0.282	
12	L,C^+ sym, P		0	0	0.288	0.295
13	L,C^+ asym, P		1	1	0.303	
14	V asym		4	4	0.323	0.325
15	T asym		1	1	0.333	
16	V sym		5	5	0.396	0.400
17	(L),C^+ sym, P		(2)	2	0.421	0.418
18	C^- sym		-	2	0.430	
19	(L),C^+ asym, P		(2)	3	0.476	
20	V asym		6	6	0.479	0.485
21	C^- asym		-	3	0.490	
22	T sym		2	2	0.501	
23	L,C^+ sym, P		2	4	0.543	0.524
24	V sym		7	7	0.568	0.576
25	C^- sym		-	4	0.605	
26	L,C^+ sym, P		2	4	0.605	0.614
27	C^+ asym, P		-	5	0.649	
28	T asym, (P)		3	3	0.661	
29	V asym		8	8	0.666	0.677
30	C^- asym		-	5	0.698	
31	(L),C^+ sym, P		(2)	6	0.716	
32	(L),C^+ asym, P		(2)	7	0.768	
33	V sym		9	9	0.772	0.787
34	C^- sym		-	6	0.807	
35	T sym		4	4	0.828	
36	C^+ sym, P		-	8	0.846	
37	Long	FS	-		0.876	
38	V asym		10	10	0.887	0.907
39	C^- asym		-	7	0.911	
40	L,C^+ asym, P		3	9	0.934	
41	L,C^+ asym, P		3	9	0.950	
42	T asym		5	5	0.992	

key to Table 1:

L	Lateral; (L) weak lateral component
P	Tower (pylon) lateral mode
V	Vertical mode
Long	Longitudinal mode
T	Torsional mode
C^+	Cable mode: cables in phase
C^-	Cable mode: cables in antiphase
FS	appears in FS variant only
SS	appears in SS variant only

Table 3 Maximum asynchronous response values for European long span box-girder suspension bridges

		Maximum displacement (cm) in:				Maximum deck bending moment (10^6Nm)		Maximum tower bending moment (10^6Nm)		Maximum shear force (10^6N) in:				Maximum axial force in tower (10^6N)	
		deck		tower		calculated	permissible	calculated	permissible	deck		tower			
vertical input	Fatih	81	(83)	13.4	(25)	46	(78)	290	59	(20)	715	1.19	(80)	0.66	(24)	19	(88)
	Bogazici	99.2	(81)	23.2	(17)	39	(76)	205	110	(25)	640	1.45	(52)	2.3	(19)	36	(25)
	Humber	92		18	(38)	75	(71)	213	350	(38)	1120	1.72	(80)	9.3	(37)	25.6	(66)
longitud -inal input	Fatih	338	(13)	39	(76)	80	(50)	290	198	(22)	715	1.52		2.28	(62)	64.4	(13)
	Bogazici	425	(13)	57		59.5	(80)	205	500		640	4.1		11.05	(99)	61.2	(74)
	Humber	287	(21)	80	(86)	152	(73)	213	1560	(83)	1120	3.18		38	(79)	55	
lateral input	Fatih	55	(54)	29.8		640	(66)	1640	270	(74)	5200	6.7	(53)	2.3	(84)	-	
	Bogazici	56	(55)	52.5	(92)	395	(49)	950	2700	(90)	13900	4.1		2	(80)	-	
	Humber	128		64.5	(89)	825		650	9760	(80)	14400	9.05		83	(80)	-	

Figures in brackets where given are values for conventional (infinite velocity) analysis as percentage of maximum values from asynchronous analysis; otherwise infinite velocity case gives maximum response value.

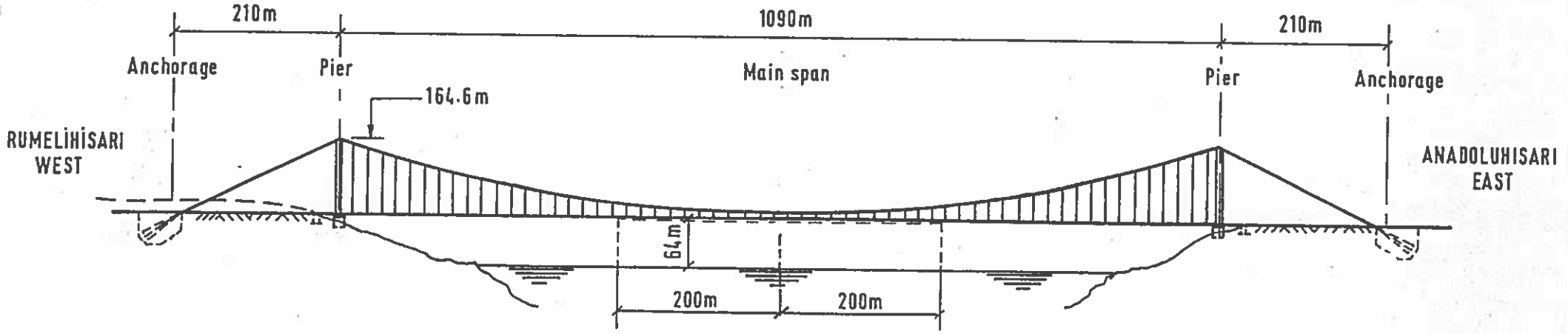

ELEVATION

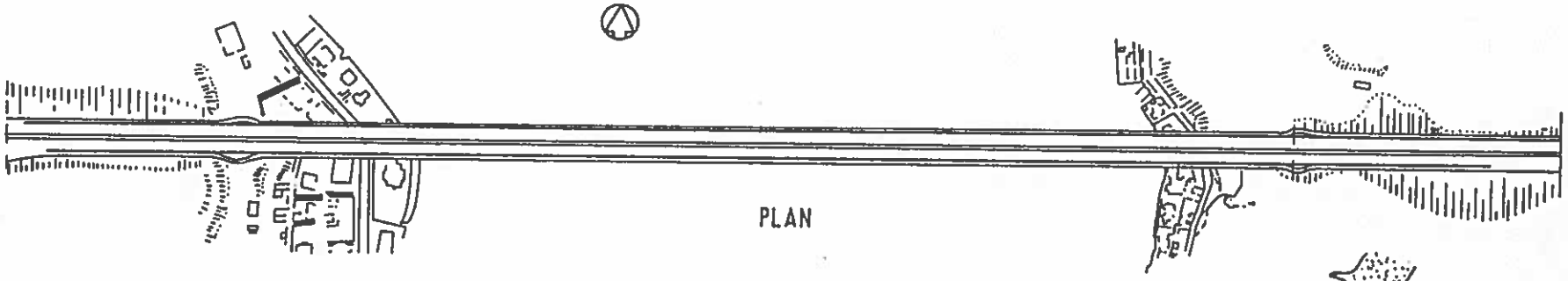

PLAN

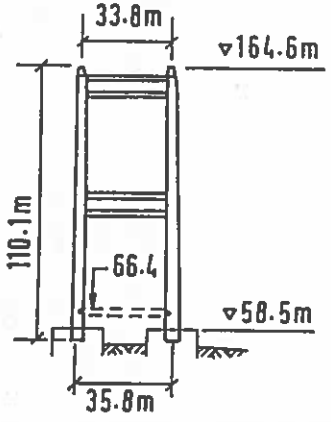

ELEVATION OF TOWERS

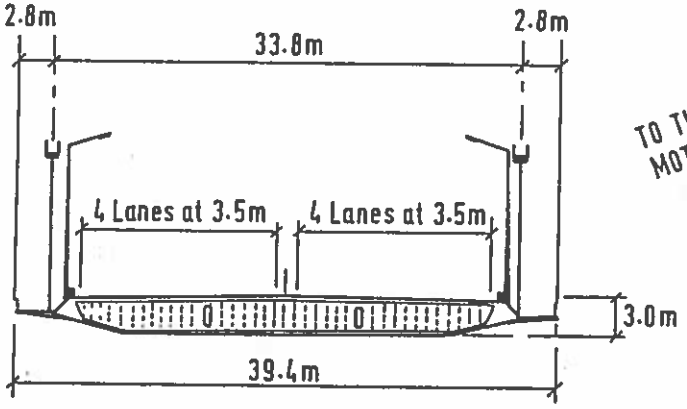

SECTION THROUGH DECK

Fig. 1

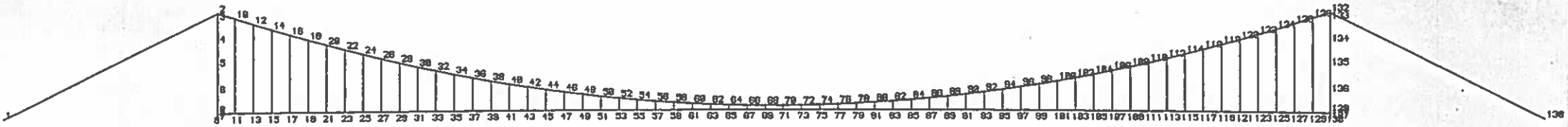

Fig. 2

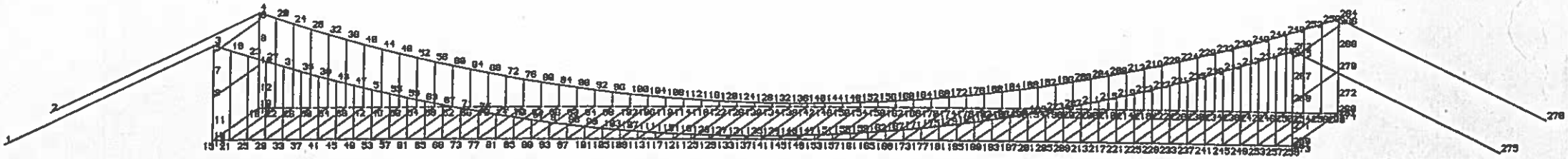

Fig. 3

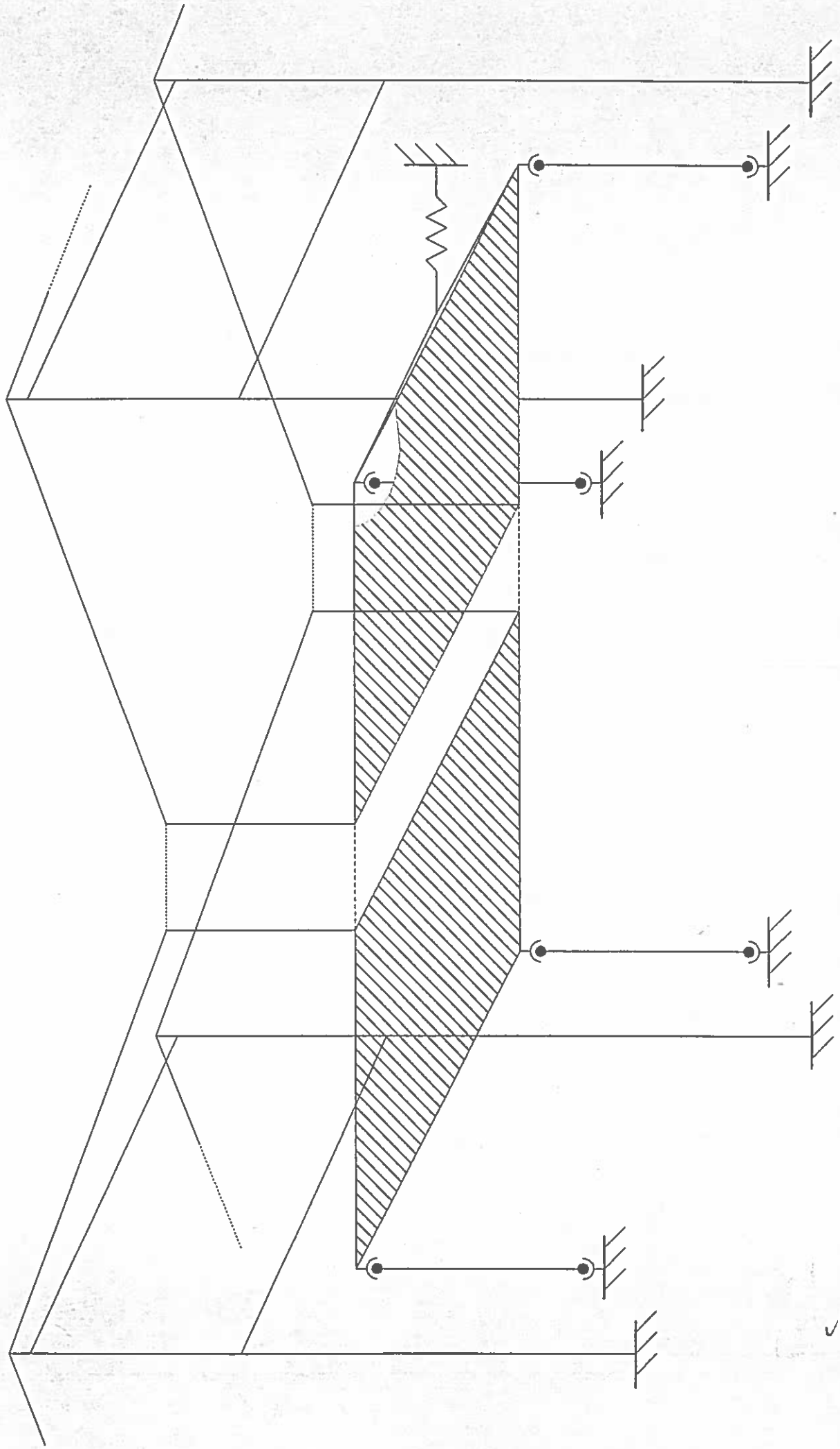

Fig. 4

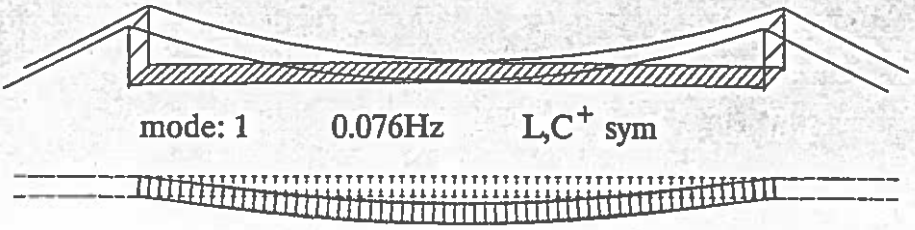

mode: 1 0.076Hz L,C^{+} sym

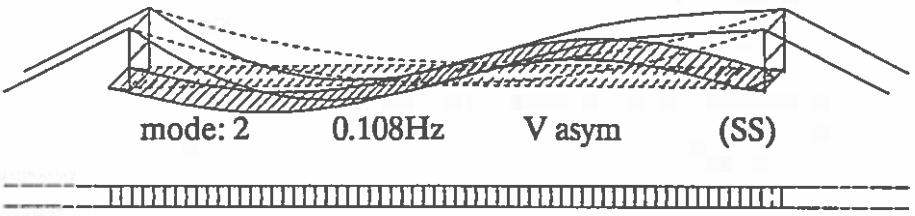

mode: 2 0.108Hz V asym (SS)

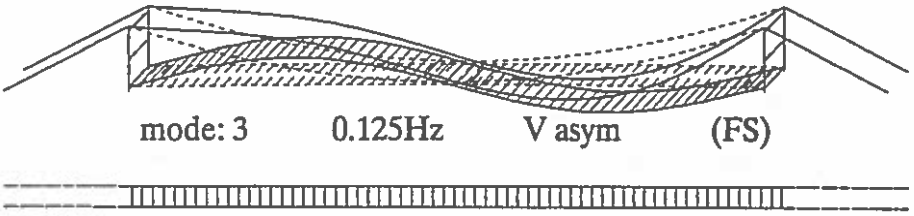

mode: 3 0.125Hz V asym (FS)

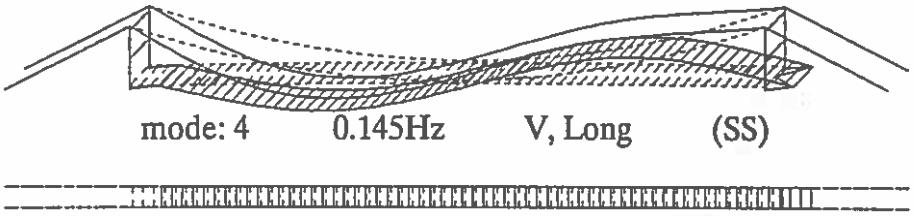

mode: 4 0.145Hz V, Long (SS)

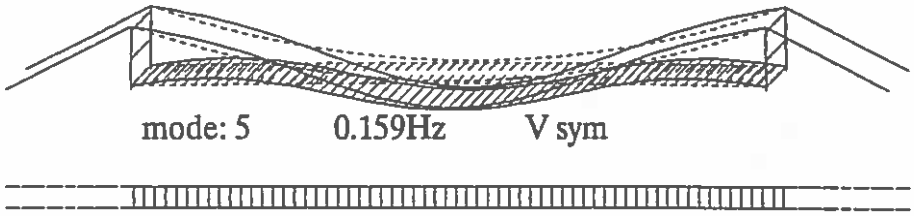

mode: 5 0.159Hz V sym

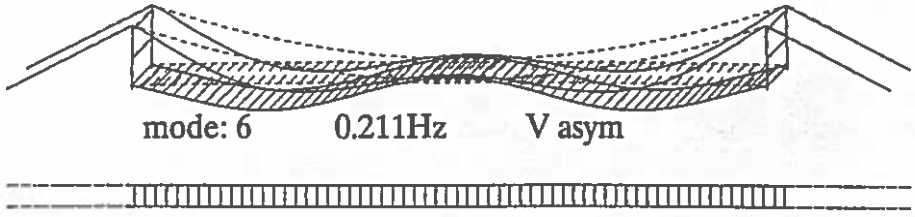

mode: 6 0.211Hz V asym

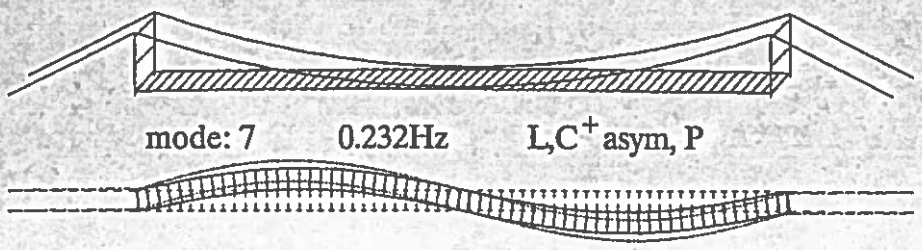

mode: 7 0.232Hz L,C^{+} asym, P

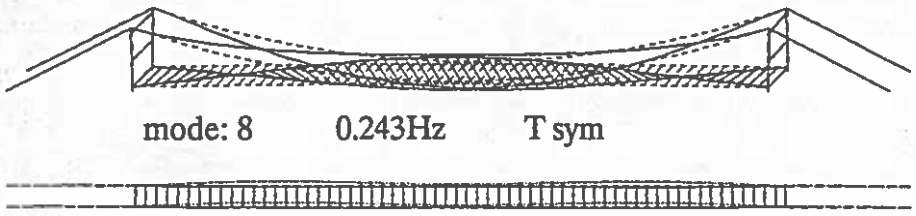

mode: 8 0.243Hz T sym

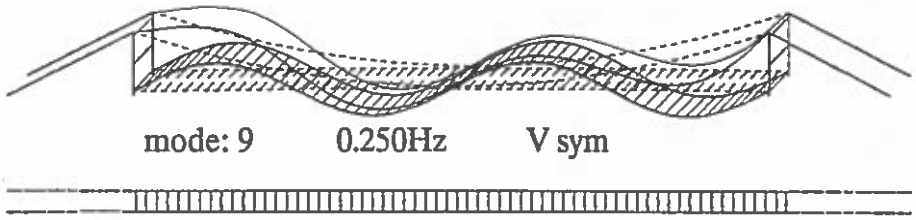

mode: 9 0.250Hz V sym

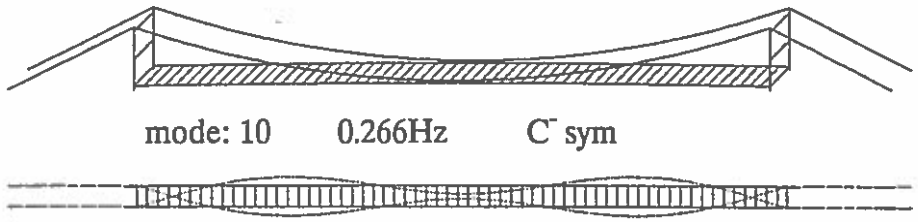

mode: 10 0.266Hz C^{-} sym

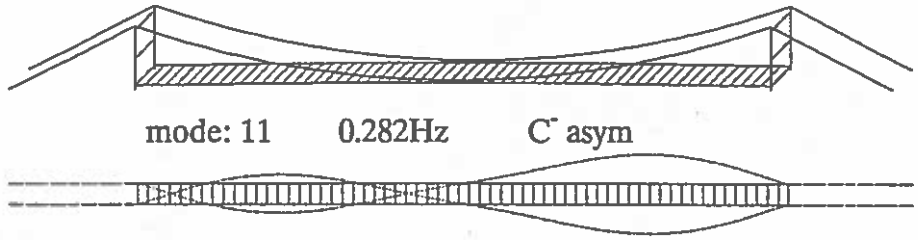

mode: 11 0.282Hz C^{-} asym

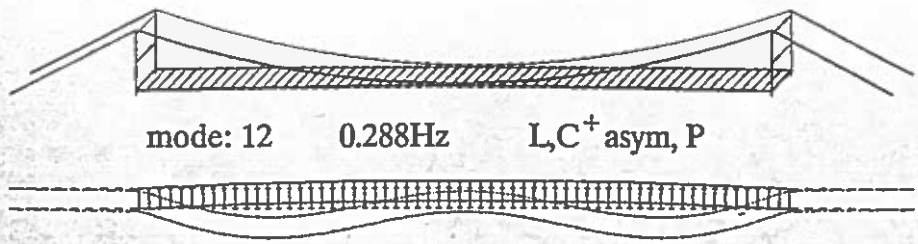

mode: 12 0.288Hz L,C^{+} asym, P

Fig 5.23

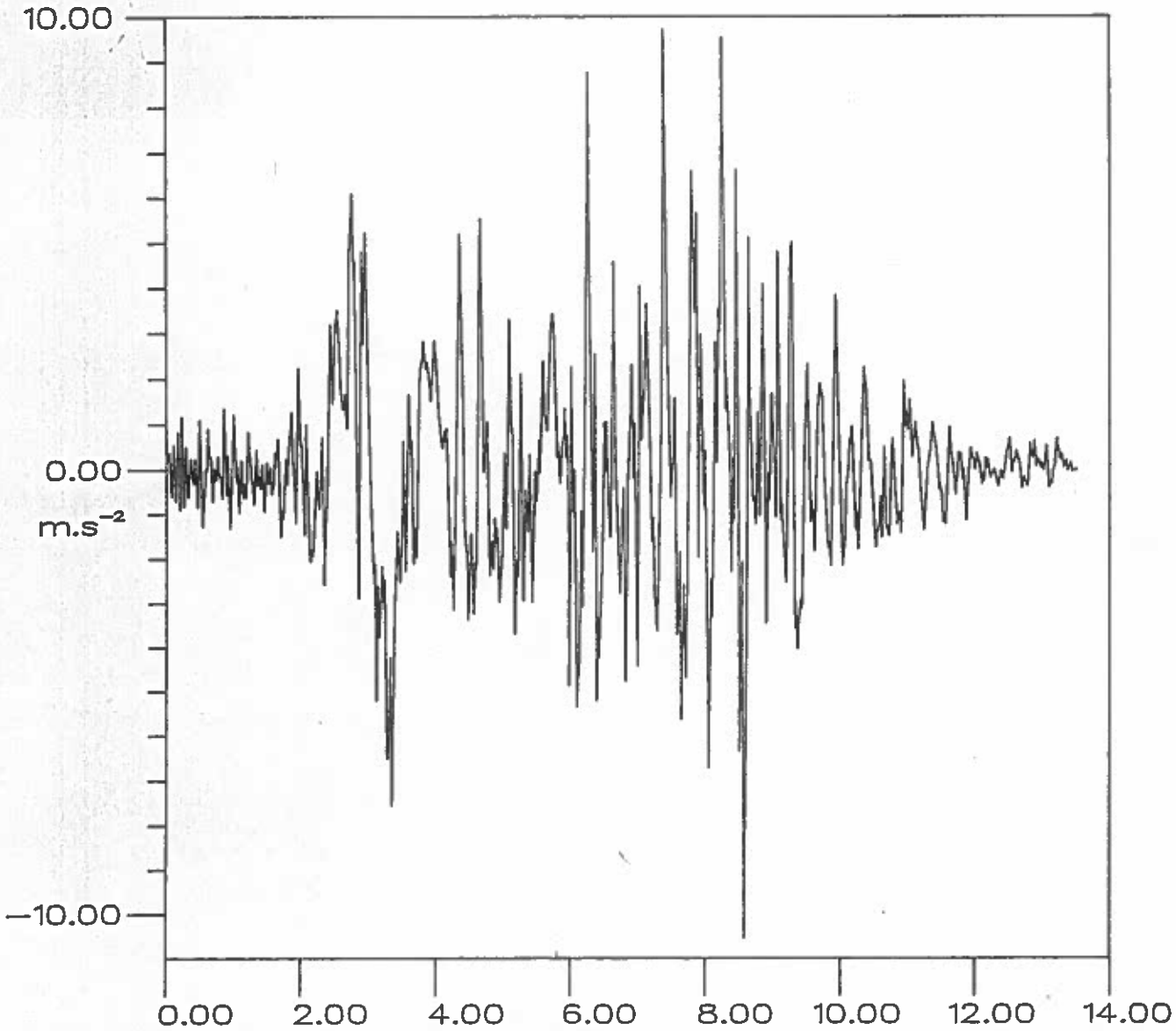

Fig. 6a

S16E acceleration time history

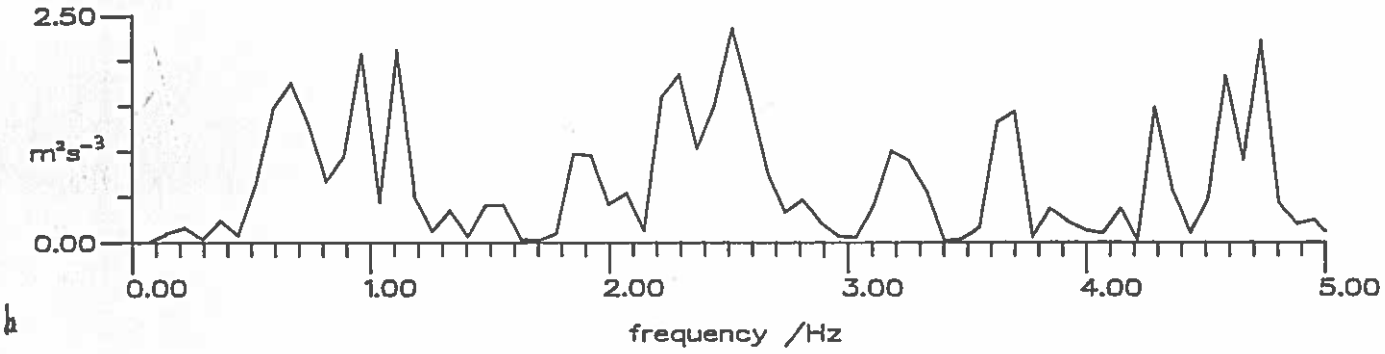

Fig. 6b

Acceleration power spectral density

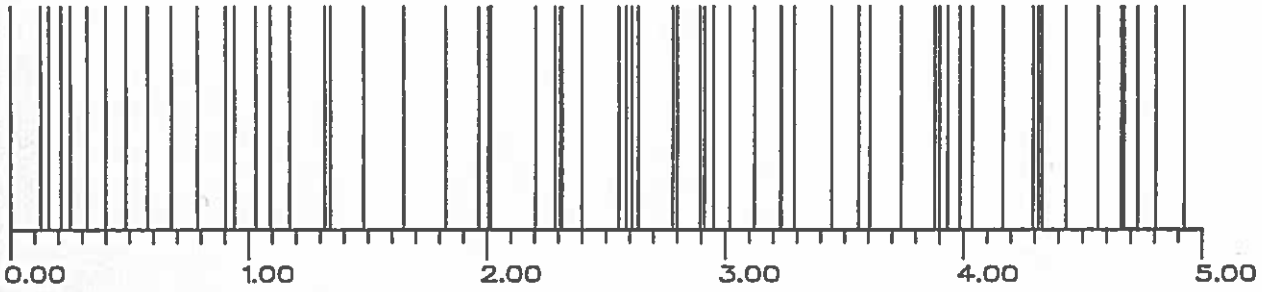

Fig. 6c

Fatih Bridge vertical modes

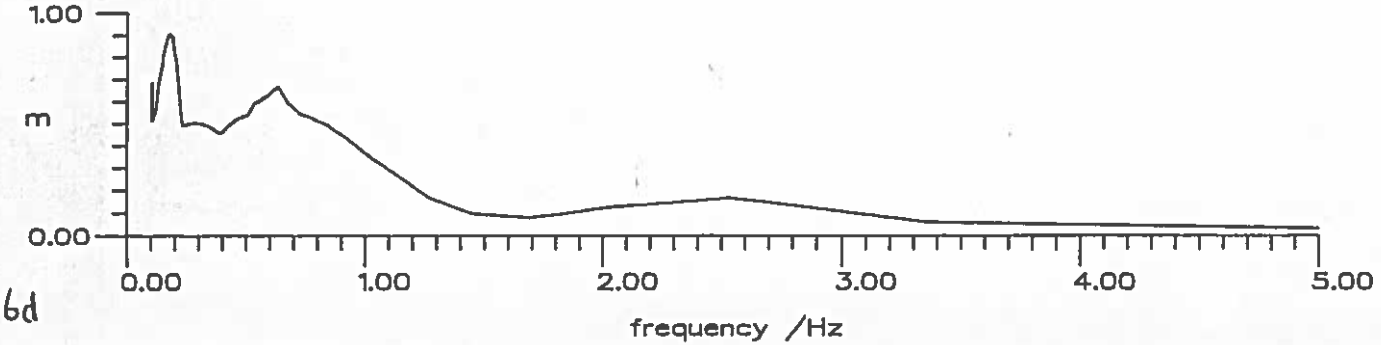

Fig. 6d

S16E displacement response spectrum; 2.5% damping

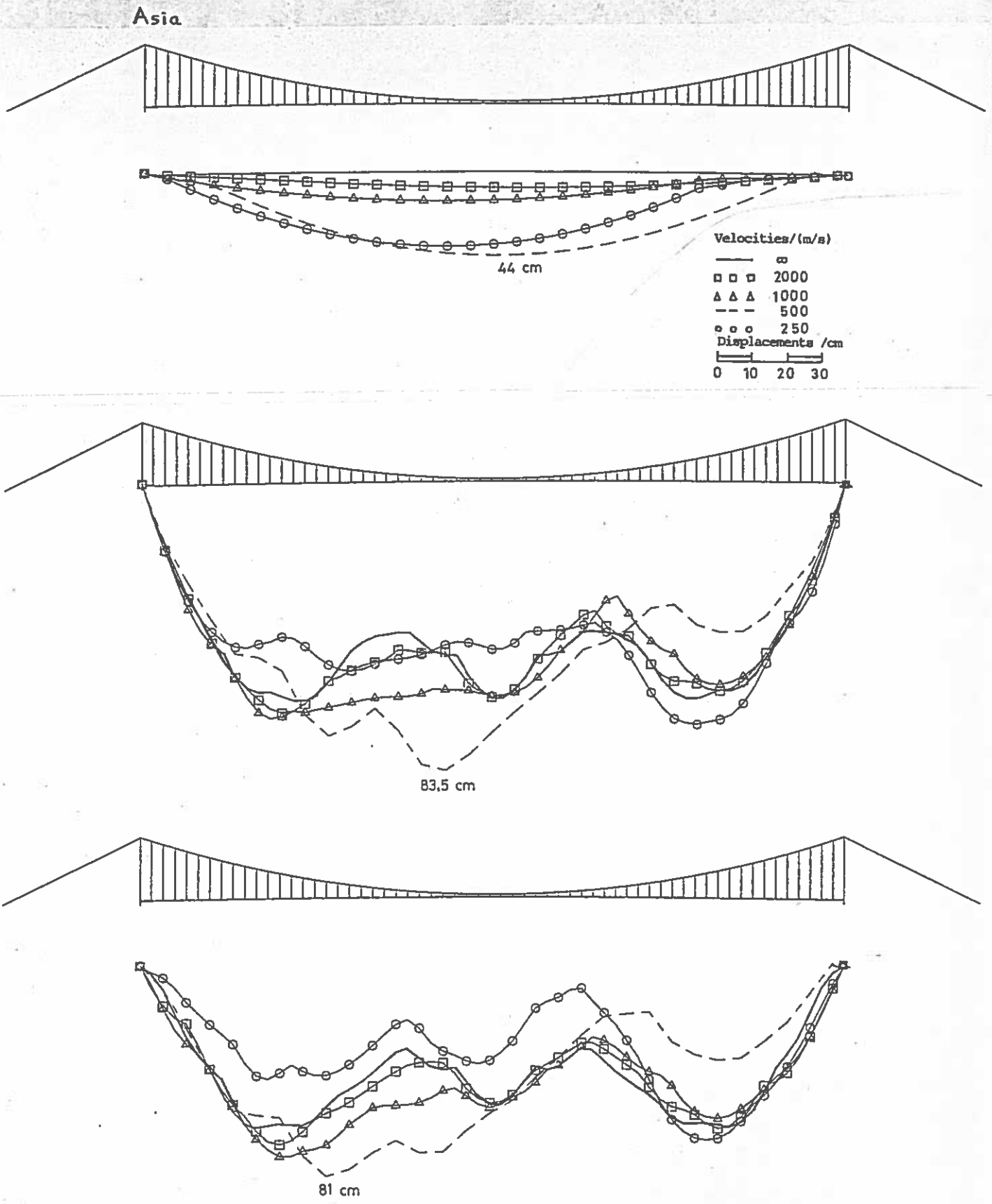
Asia
a)
44 cm
Velocities/(m/s)
∞
2000
1000
500
250
Displacements /cm
0 10 20 30
b)
83,5 cm
c)
81 cm

Fig. 7

Fig. 8

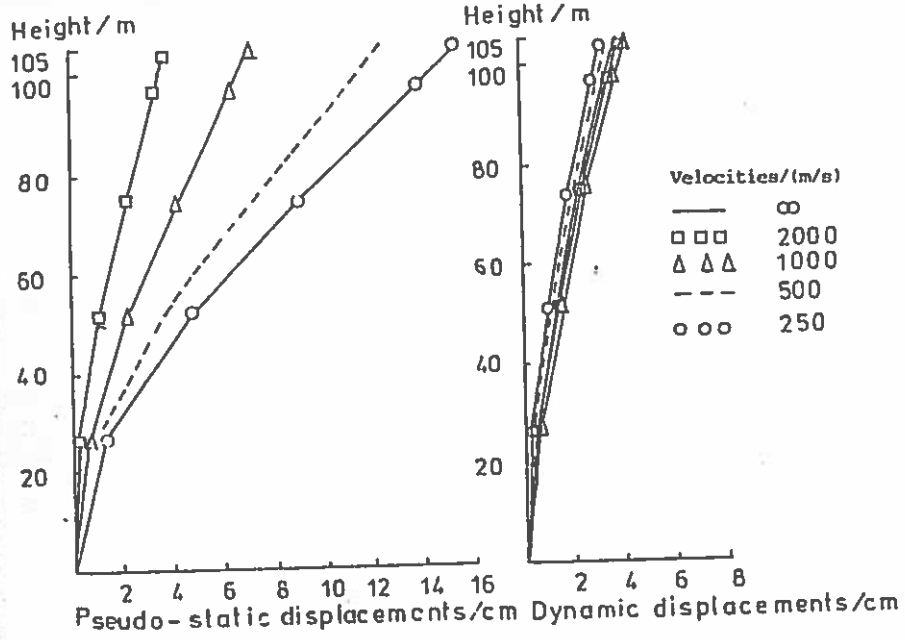
Height / m
105
100
80
60
40
20
2 4 6 8 10 12 14 16
Pseudo-static displacements/cm
Height / m
105
100
80
60
40
20
2 4 6 8
Dynamic displacements/cm
Velocities/(m/s)
∞
2000
1000
500
250

a b

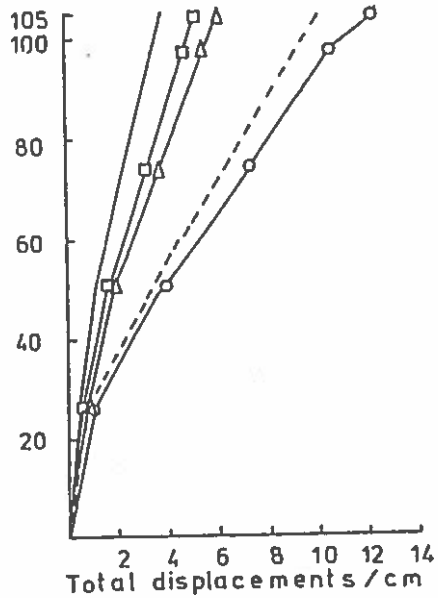
105
100
80
60
40
20
2 4 6 8 10 12 14
Total displacements / cm

c

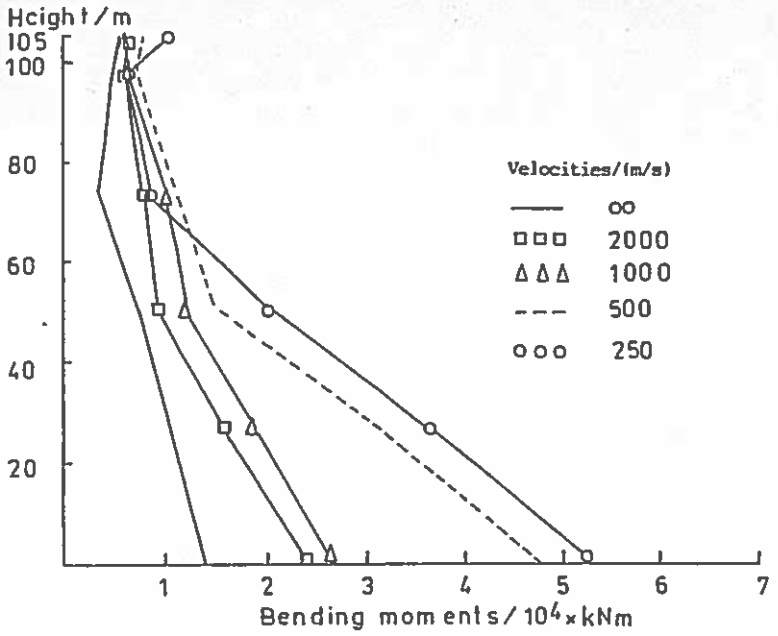
Height / m
105
100
80
60
40
20
Velocities/(m/s)
∞
2000
1000
500
250
1
2
3
4
5
6
7
Bending moments / 10^4 × kNm

Fig. 9

a)

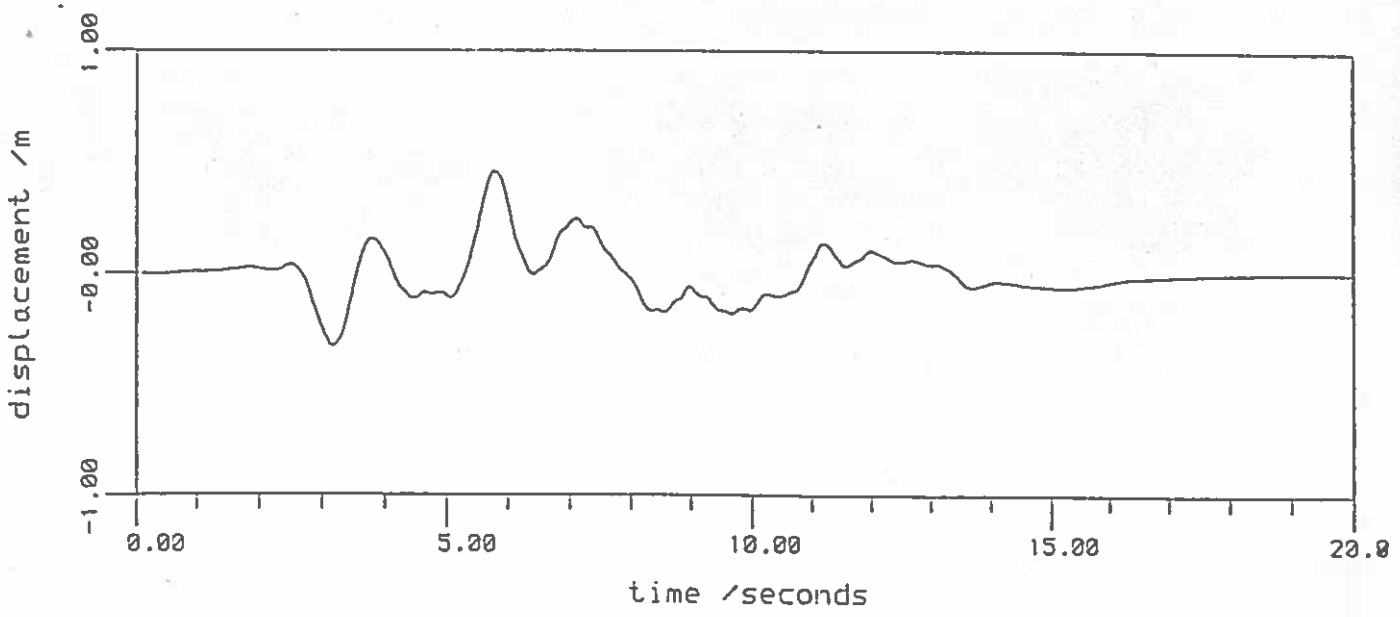
displacement /m
1.00
-0.00
-1.00
0.00
5.00
10.00
15.00
20.0
time /seconds

b)

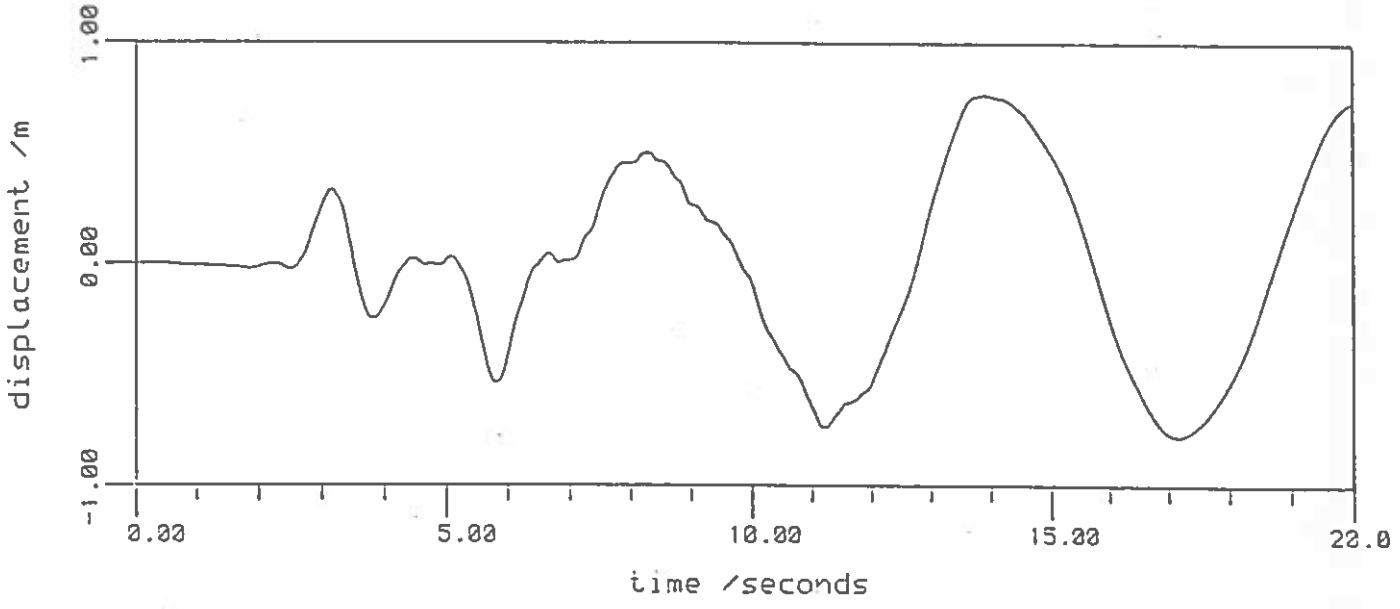
displacement /m
1.00
0.00
-1.00
0.00
5.00
10.00
15.00
20.0
time /seconds

c)

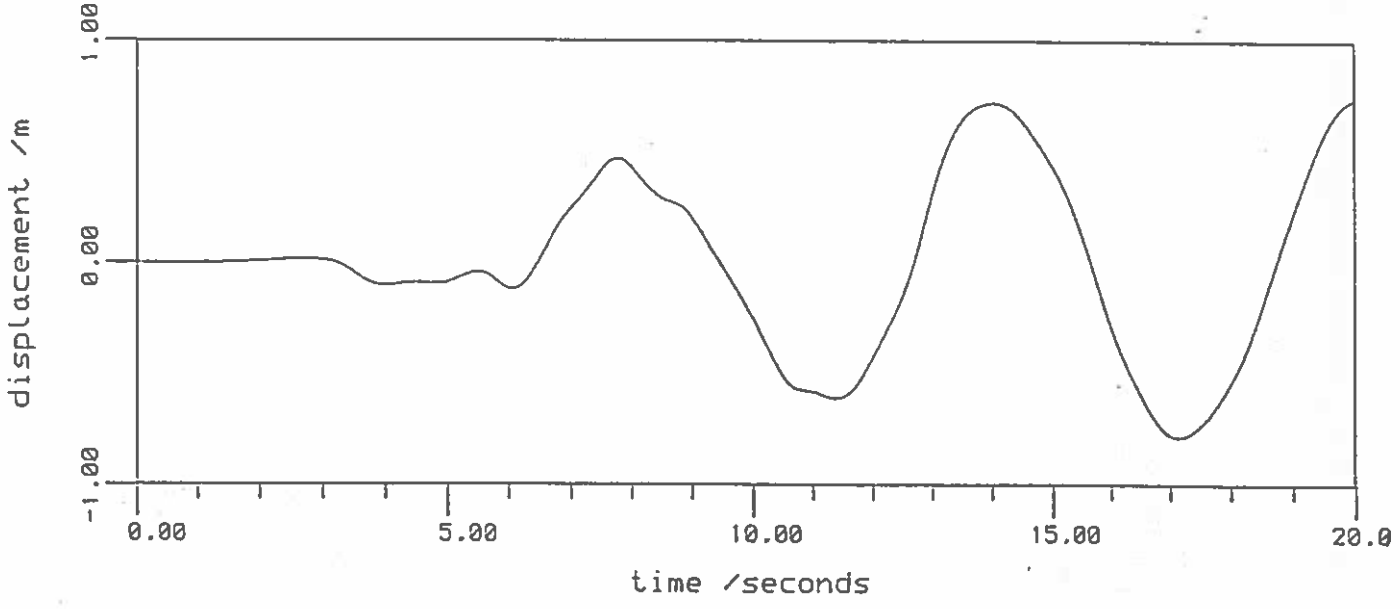
displacement /m
1.00
0.00
-1.00
0.00
5.00
10.00
15.00
20.0
time /seconds

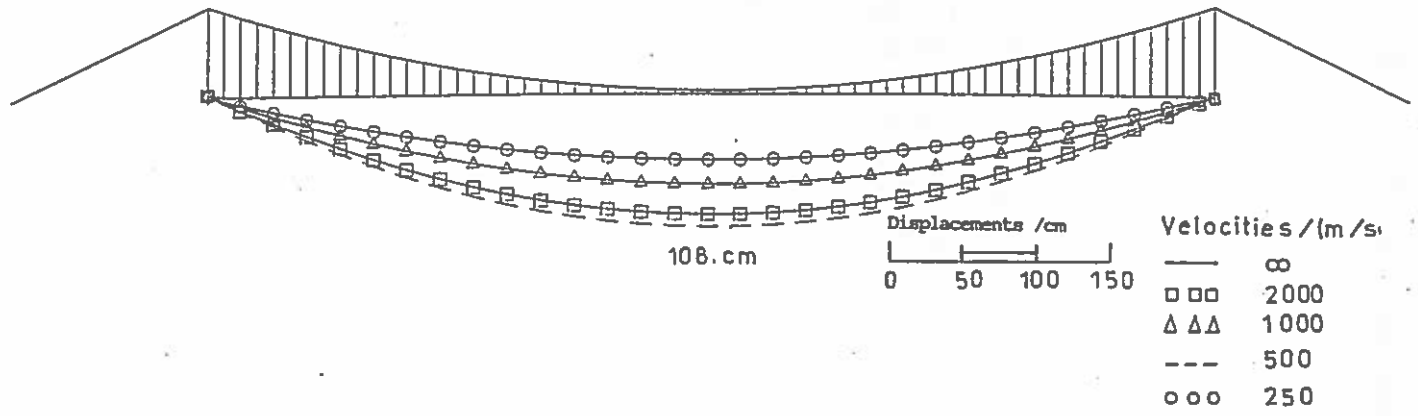

108.cm

)

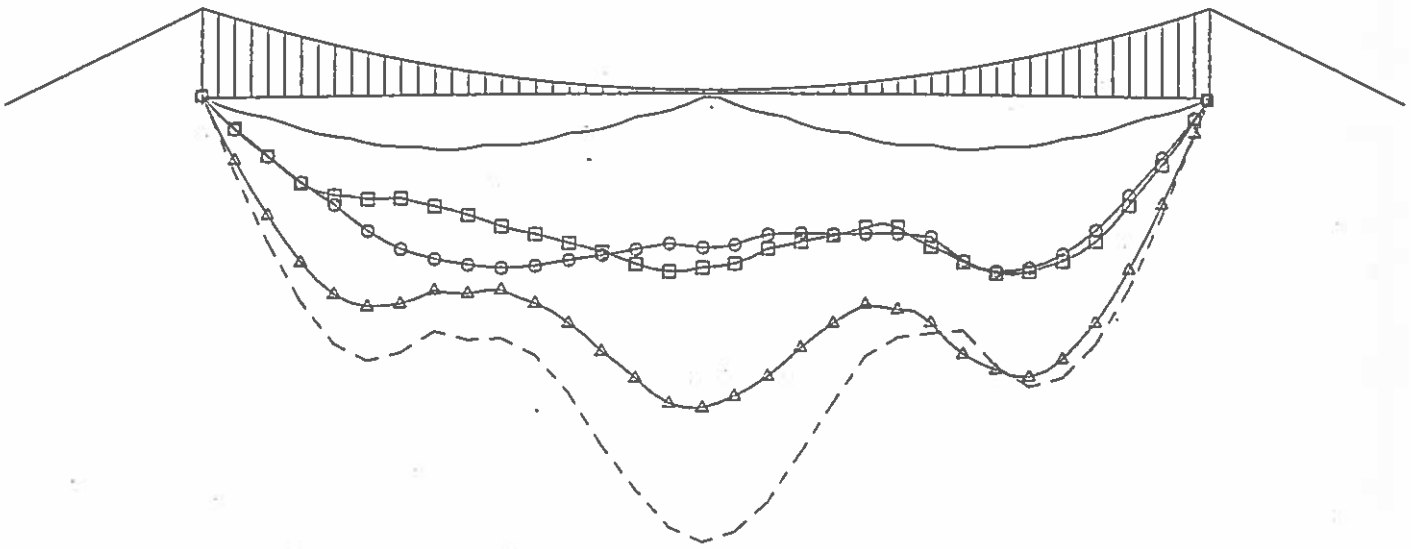

b)

364cm

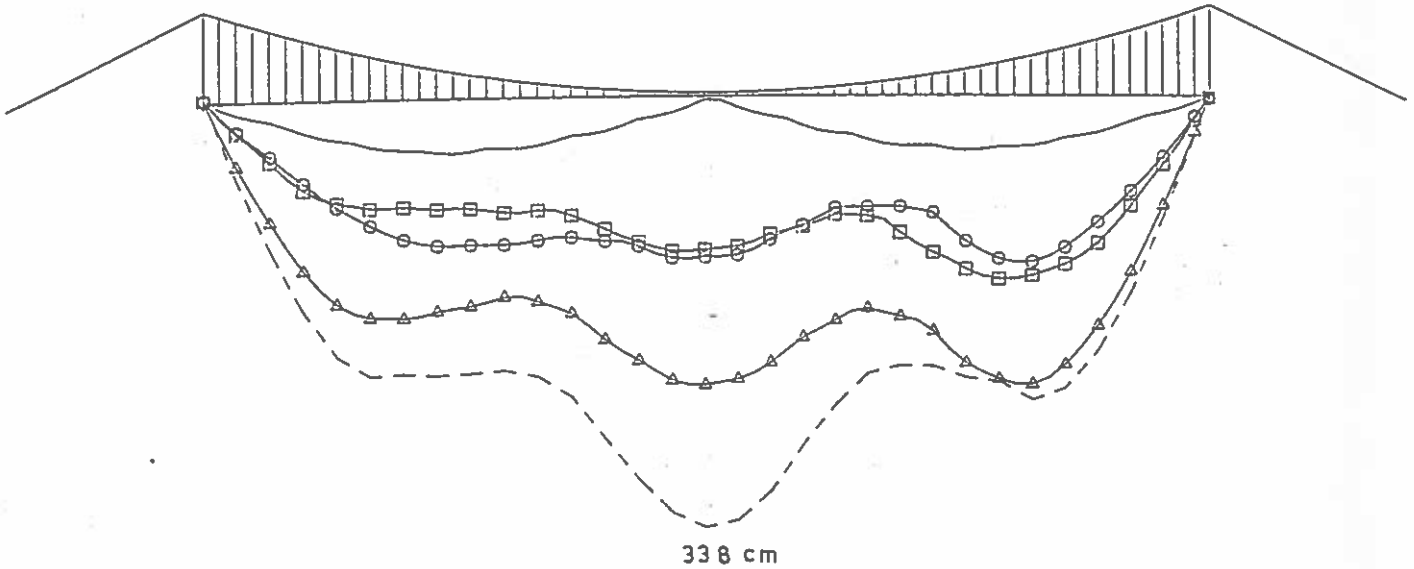

c)

338 cm

Fig. 11

Fig. 12

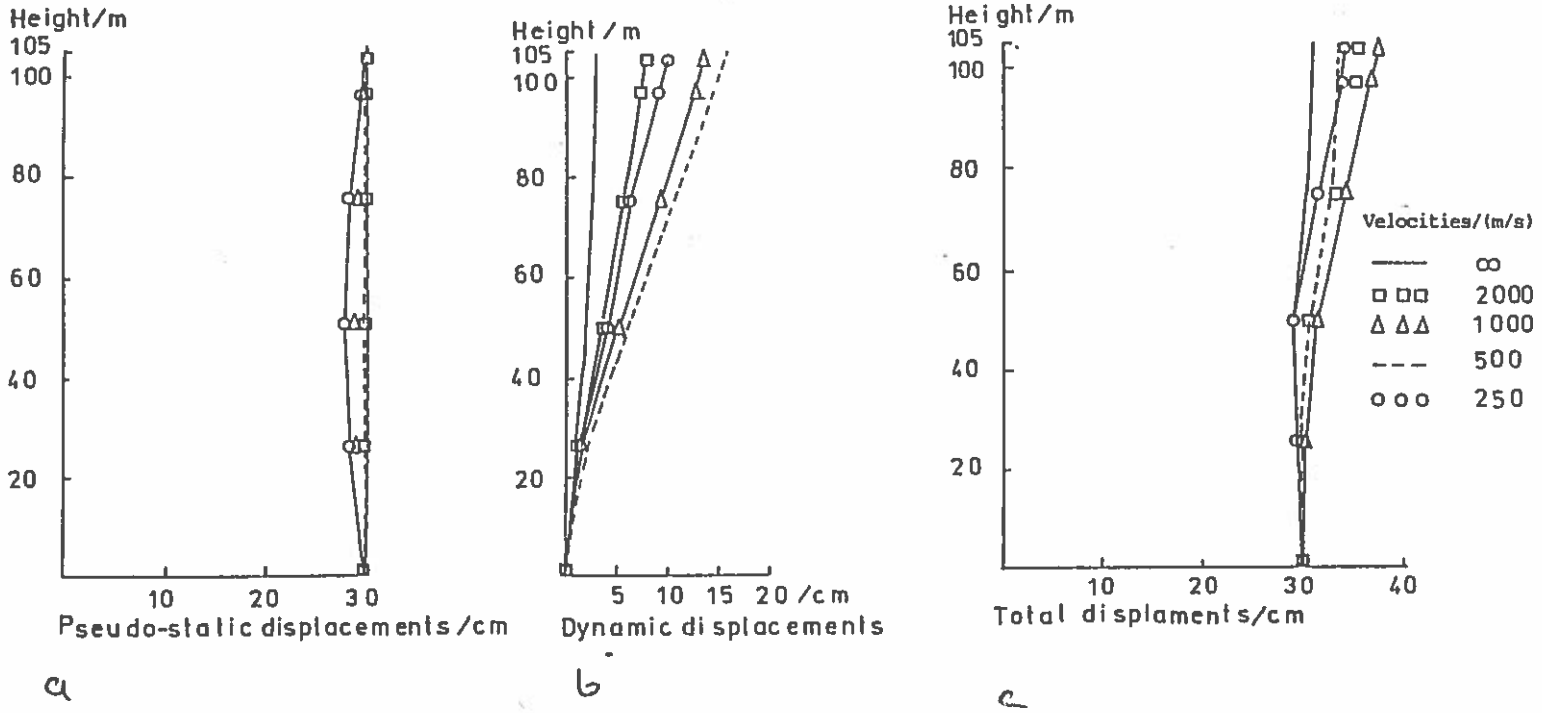
Height/m
105
100
80
60
40
20
10
20
30
Pseudo-static displacements/cm
a
Height/m
105
100
80
60
40
20
5
10
15
20 /cm
Dynamic displacements
b
Height/m
105
100
80
60
40
20
10
20
30
40
Total displaments/cm
c
Velocities/(m/s)
∞
2000
1000
500
250

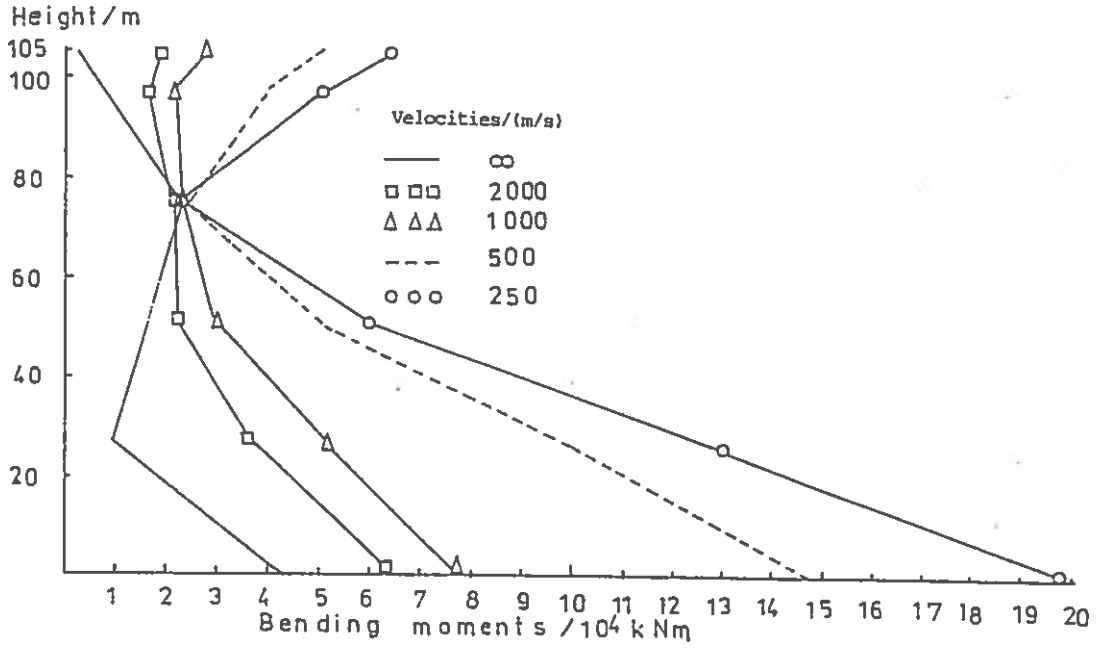
Height/m
105
100
80
60
40
20
Velocities/(m/s)
∞
2000
1000
500
250
1 2 3 4 5 6 7 8 9 10 11 12 13 14 15 16 17 18 19 20
Bending moments /10⁴ kNm

Fig. 13

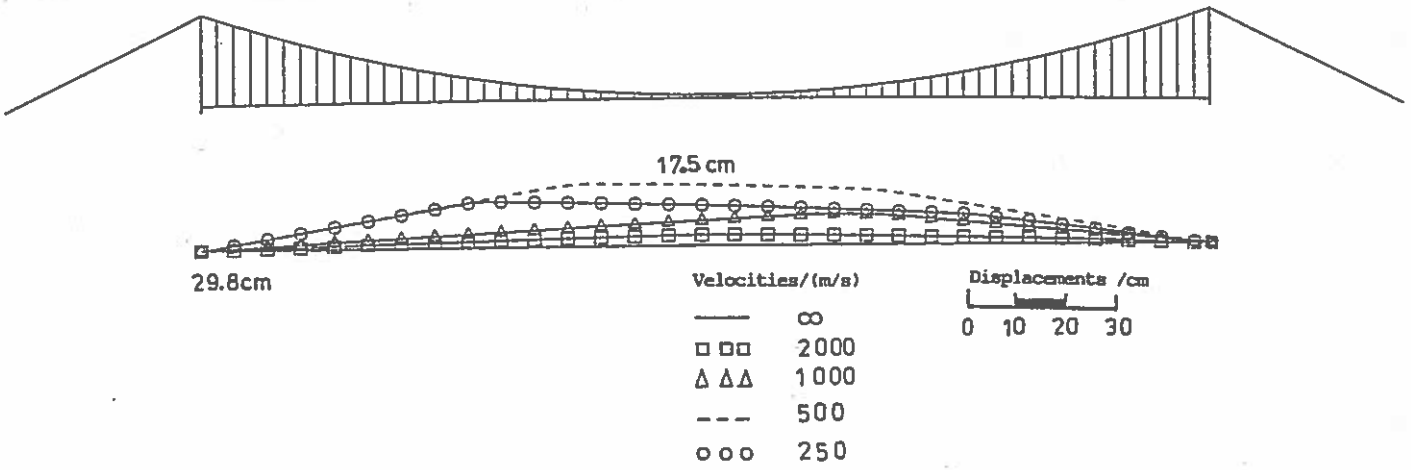
17.5 cm
29.8cm
Velocities/(m/s)
∞
2000
1000
500
250
Displacements /cm
0 10 20 30

1)

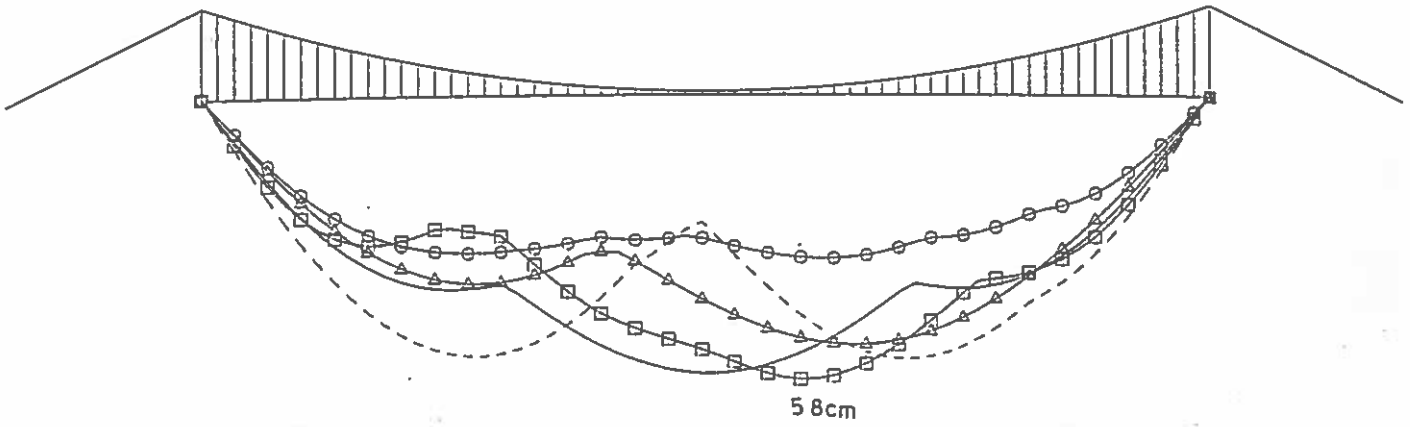
5.8cm

b)

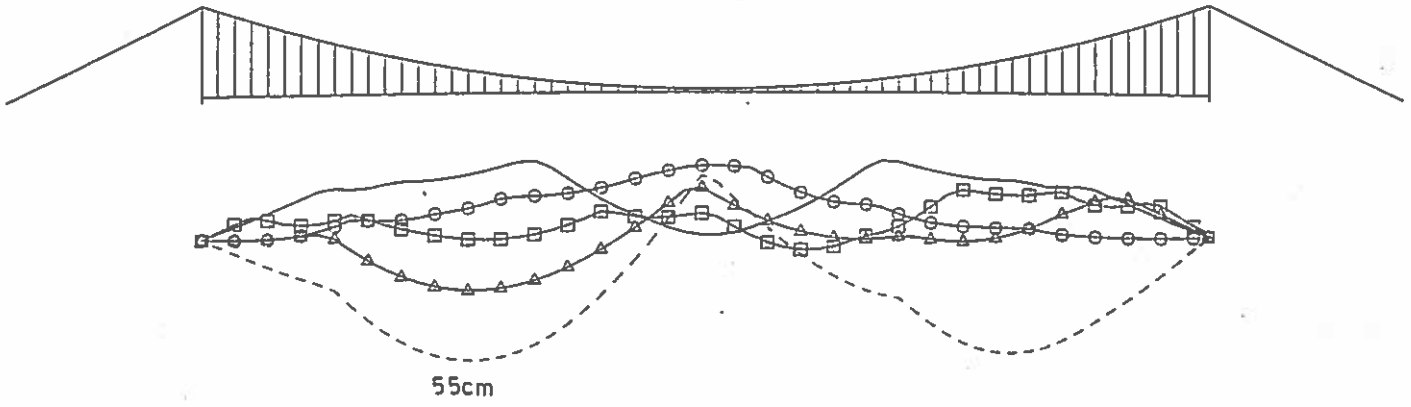
55cm

c)

Fig. 14

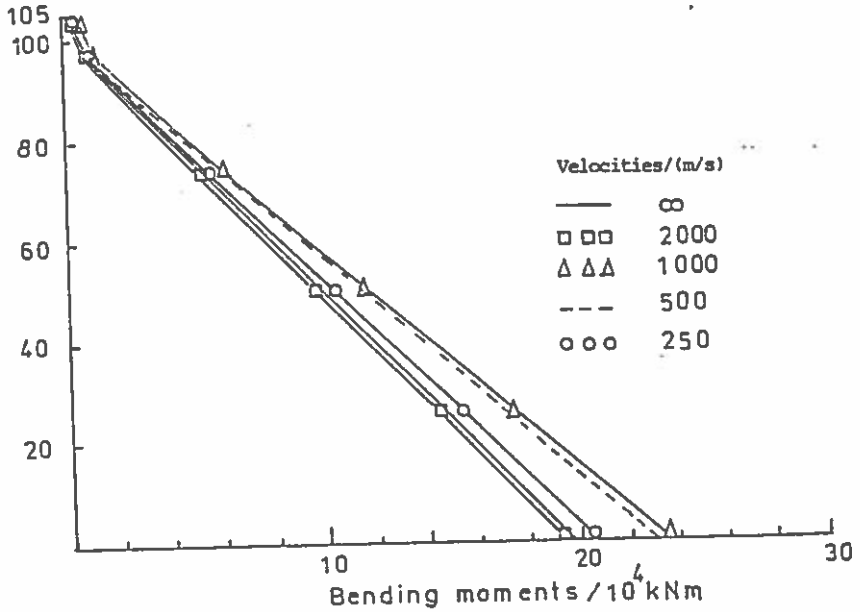
105
100
80
60
40
20
10
20
30
Bending moments / 10⁴ kNm
Velocities/(m/s)
∞
2000
1000
500
250

Fig. 15

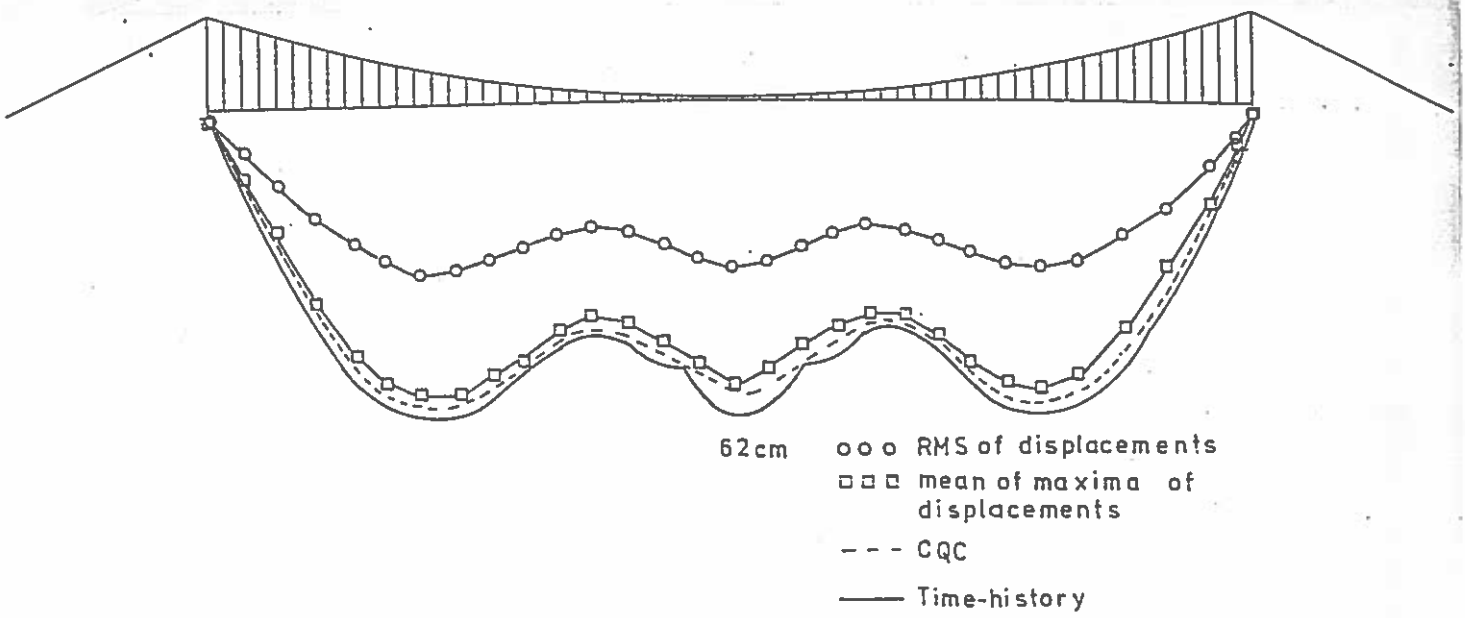
62cm
ooo RMS of displacements
□□□ mean of maxima of displacements
--- CQC
—— Time-history

a

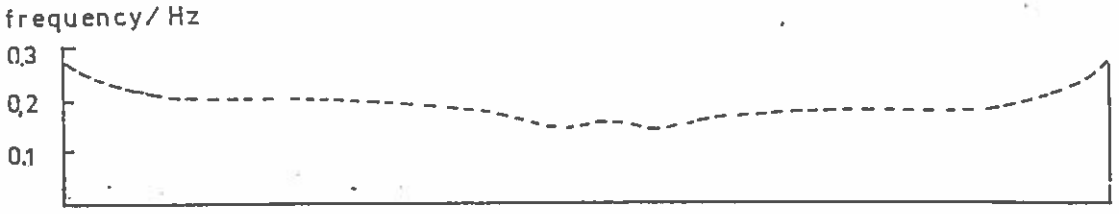
frequency/ Hz
0.3
0.2
0.1

b

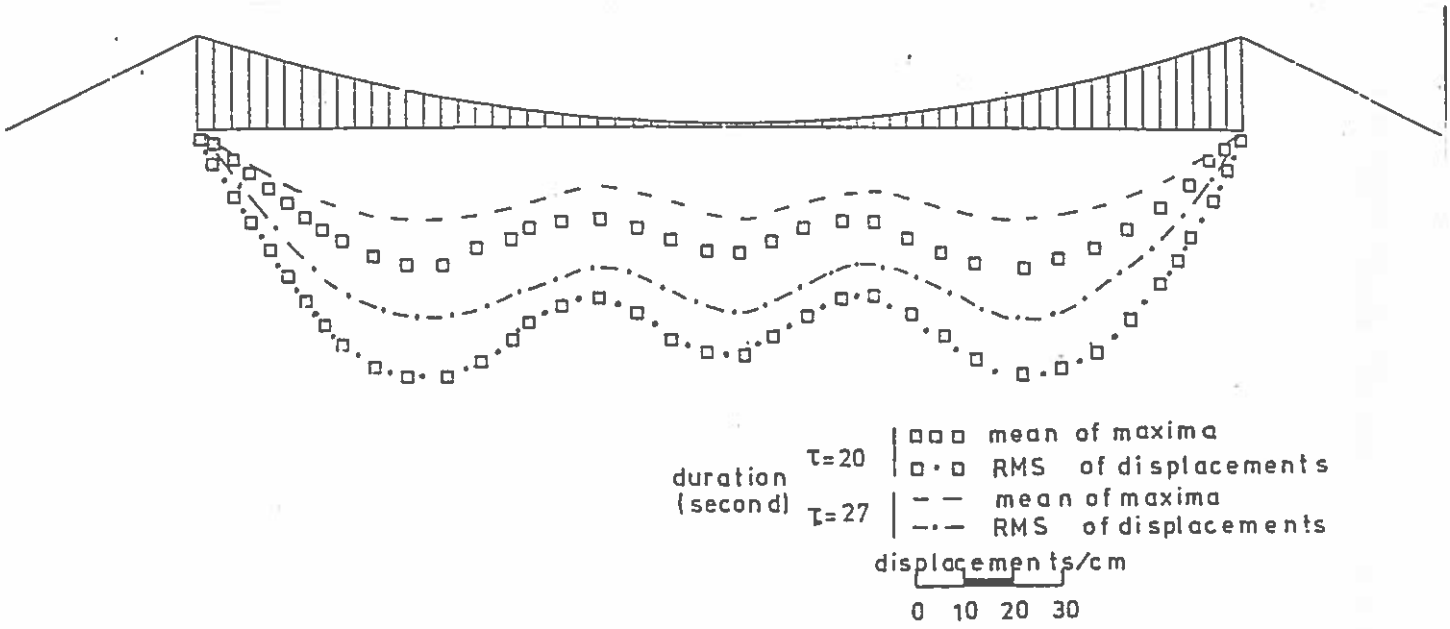
duration (second)
τ=20
□□□ mean of maxima
□·□ RMS of displacements
τ=27
– – mean of maxima
–·– RMS of displacements
displacements/cm
0 10 20 30

c

Fig 16

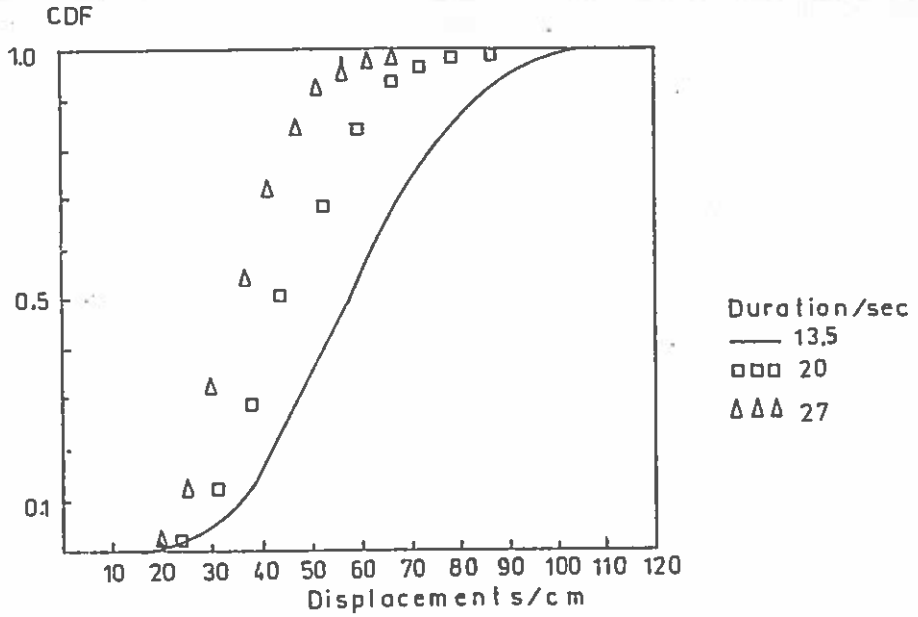
CDF
1.0
0.5
0.1
10 20 30 40 50 60 70 80 90 100 110 120
Displacements/cm
Duration/sec
13,5
20
27

a)

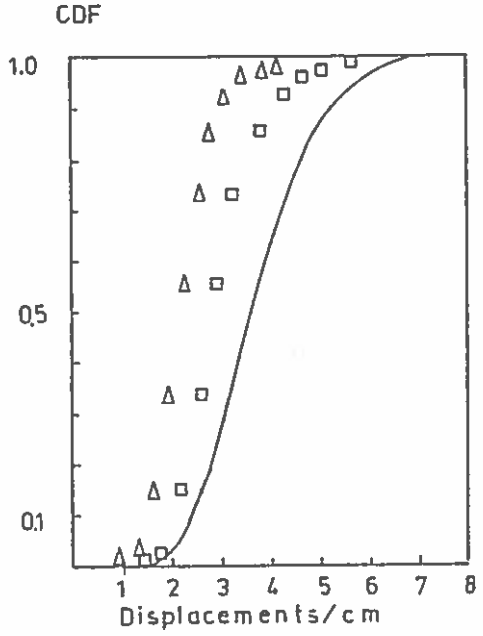
CDF
1.0
0,5
0.1
1 2 3 4 5 6 7 8
Displacements/cm

b)

Fig. 17

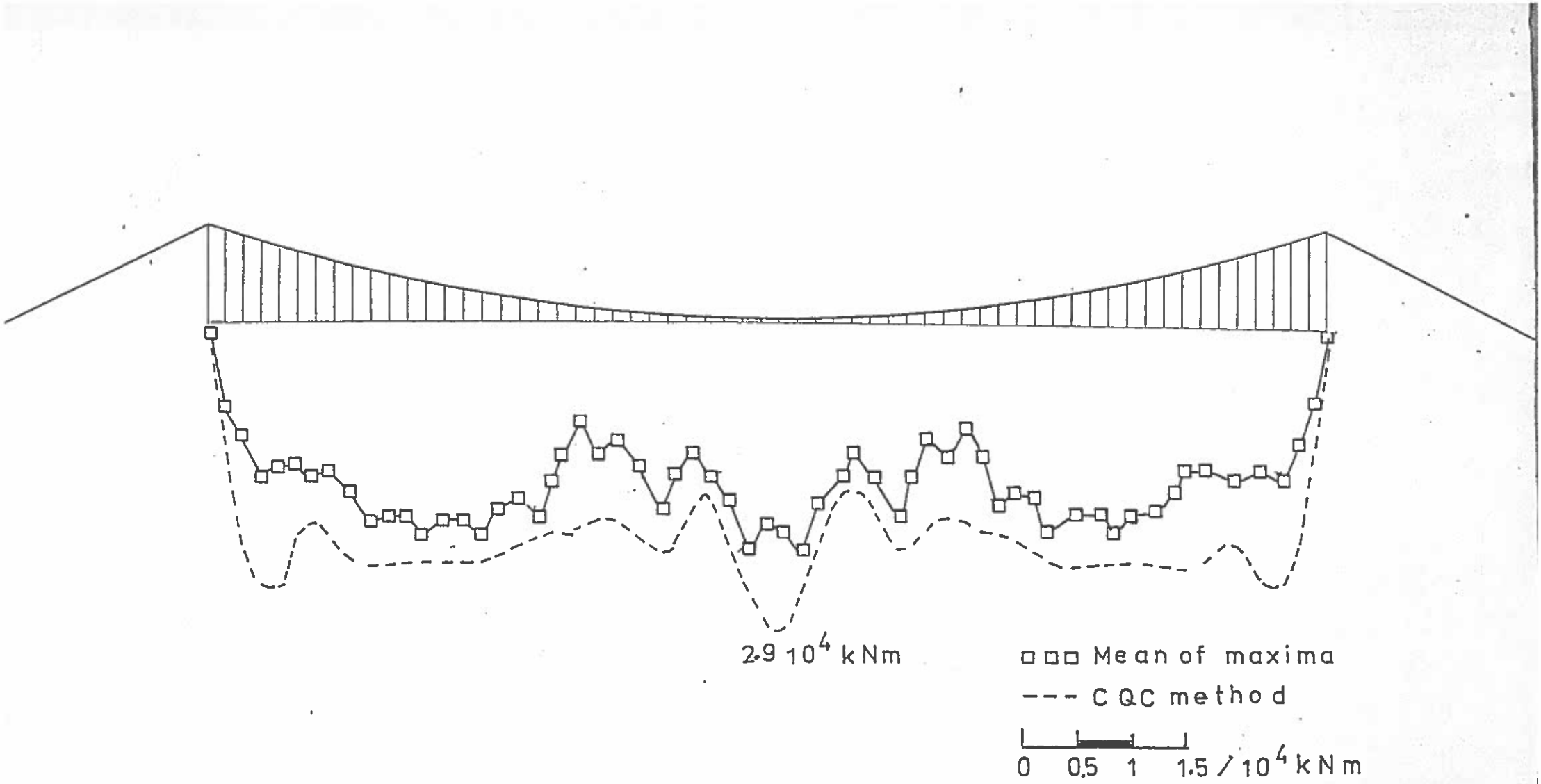

Fig. 18